

Novel Charged Microcapsules as Templates for Layer-by-Layer Assembly of Polyelectrolytes and Adsorption of Lipid Bilayers

Master of Science Thesis in the Master Degree Program Chemistry and Biosciences

YE LI

Department of Chemical and Biological Engineering
Division of Applied Chemistry
CHALMERS UNIVERSITY OF TECHNOLOGY
Göteborg, Sweden 2011
Report No.

Novel Charged Microcapsules as Templates for Layer-by-Layer Assembly of Polyelectrolytes and Adsorption of Lipid Bilayers

Master of Science Thesis in the Master Degree Program Chemistry and Biosciences

Ye Li



Supervisors: Magnus Nydén & Markus Andersson Trojer
Examiner: Magnus Nydén

Department of Chemical and Biological Engineering
CHALMERS UNIVERSITY OF TECHNOLOGY
Göteborg, Sweden 2011

Novel Charged Microcapsules as Templates for Layer-by-Layer Assembly of Polyelectrolytes and Adsorption of Lipid Bilayers

Ye Li

© Ye Li, 2011.

Report No.
Department of Chemical and Biological Engineering
Chalmers University of Technology
SE-412 96 Göteborg
Sweden

Telephone +46 (0) 31-772 1000

Cover: SEM image of microcapsules synthesized with PMMA(600)-b-PMANa(4600) as emulsifier.

Department of Chemical and Biological Engineering
Göteborg, Sweden 2011

Abstract

Fouling of marine organisms such as barnacles on the ship hull surface is a severe problem for the shipping industry. It greatly increases the friction drag between the ship and the sea water. More fuel is needed which results in more pollution to the environment. Therefore antifouling agents, i.e. biocides, are used in the marine paint in order to prevent the fouling. However, the lifetime of the paint is too short due to the premature release of the biocides. Encapsulation of the biocides in poly(methyl methacrylate) microcapsules is an efficient way to reduce the release and protect the biocides. However, given the long expected lifetime of the marine coating (five years), the release from the microcapsules is still too fast. Another important problem is the poor colloidal stability of the capsules, preventing the capsules to be dispersed in the paint formulation as dried powder.

The aim of this project is to increase the colloidal stability of the microcapsule system and also to reduce the release rate of biocides from microcapsules.

The colloidal stability may be increased by using charged microcapsules and the charges may be introduced by using ionic emulsifiers. Regarding the release, the use of an additional hydrophilic layer on the microcapsule may act as a good barrier against the typically rather hydrophobic biocides. Polyelectrolyte multilayers are promising hydrophilic barriers which may be accomplished using layer by layer assembly on the charged microcapsules. Beyond this, lipid bilayers on the surface of microcapsules may be another way to reduce the release rate due to the tight packing of the lipids in the crystalline phase below the phase transition temperature.

The charged microcapsules were synthesized using three different kinds of charged emulsifiers: a weak polyacid PMMA (poly(methacrylic acid)), four block copolymers PMMA-b-P(M)AA (poly(methyl methacrylate)-b-((meth)acrylic acid)) and a hydrophobic anionic surfactant TC4 in combination with a polycation PDADMAC (poly(diallyldimethyl ammonium chloride)). The characterization of these microcapsules was studied using light microscopy, Scanning Electron Microscopy (SEM), microelectrophoresis and Electron Spectroscopy for Chemical Analysis (ESCA).

The microcapsules synthesized using the weak polyacid PMAA as the emulsifier had a relatively low negative surface charge. By using amphiphilic block copolymers instead of weak polyacid, microcapsule with a high negative surface charge was obtained. With the aid of hydrophobic anionic surfactant TC4, the polycation PDADMAC was able to be adsorbed, providing the capsule with a high positive surface charge. However, these microcapsules were only stable during a couple of weeks. In addition, the liposomes could also be adsorbed on the surface of the microcapsules with opposite surface charge.

Microcapsules prepared using block copolymers or TC4-PDADMAC as emulsifiers have a higher surface charge compared to PMAA microcapsules, and are therefore more suitable for further surface modification. There's no problem to redisperse them after washing with water. The microelectrophoresis results proved that multilayers of polyelectrolytes could be adsorbed on all three types of template microcapsules.

The future work will focus on the surface modification of microcapsules with other several types of block copolymers as emulsifiers. The washing protocol for microcapsules with adsorbed lipid bilayers needs to be improved. Most importantly, the release rate of biocides from microcapsules will be studied as well, such as the difference of release rate from microcapsules synthesized with different types of emulsifiers, or the difference of release rate from pure microcapsules and microcapsules adsorbed with polyelectrolyte multilayers or lipid bilayers.

Contents

Abstract	4
Contents	6
Introduction	8
Theory	10
Microencapsulation.....	10
Microencapsulation techniques.....	10
Solvent evaporation	12
Size of the microcapsules	13
Layer-by-Layer Techniques	14
Liposomes and lipid bilayers	15
Experimental	17
Light Microscopy	17
Dark field microscopy.....	17
Microelectrophoresis	18
Experimental considerations.....	18
The electric double-layer and electrophoresis.....	19
ESCA	20
SEM	20
Material and Methods	21
Material.....	21
Emulsifier	21
Polyelectrolytes.....	22
Lipids	23
Methods.....	23
Preparation of microcapsules and microspheres.....	23
Summary of all microencapsulations	24
Polyelectrolyte Layer-by-Layer Adsorption	24
Lipid bilayer formation on charged particles.....	24
Preparation of small unilamellar vesicles (SUVs)	24
Liposome adsorption, rupture and spreading on charged particles	25
Characterization	25
Light microscopy	25
Microelectrophoresis	25
ESCA	26
Sample preparation.....	26
PMAA as emulsifier and effect of pH	26
SEM	26
Results and discussions.....	27
Characterization of microcapsules	27
Light microscopy and size distribution	27
Weak polyelectrolyte	27
Amphiphilic diblock copolymers	28

Hydrophobic anionic surfactant and polycation	31
Microelectrophoresis and ζ -potential	33
ESCA results	34
PMAA as emulsifier and effect of pH	34
Surface modification on colloidal particles	36
LbL assembly of Polyelectrolytes	36
Building lipid bilayers on the surface of microcapsule	38
Conclusion	39
Future work	40
Acknowledgement	41
Appendix I	42
Appendix II	43
Appendix III	44
Appendix IV	45
Appendix V	47
References	48

Introduction

Fouling of marine organisms, such as algae and barnacles (see Figure 1), on ships has been a serious problem for both commercial shipping and leisure boating. Once these organisms are attached to the ship's hulls, they will increase the surface roughness of the hull. Therefore, the hydrodynamic drag is increased when the ship moves through water, which adversely affects the manoeuvrability and fuel consumption ^[1].

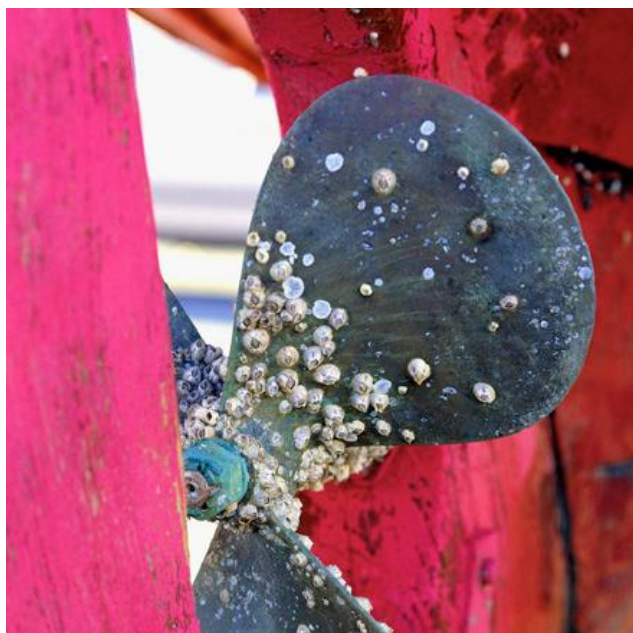


Figure 1. Barnacles: a severe fouling problem. Photo: Jan-Olof Yxell ^[2].

A six-month fouling of organisms on a ship's hull without antifouling coating can lead to a 40% increase in fuel consumption. Furthermore, the fouling increases the costs for maintenance, including dry-docking, surface treatment and / or repainting ^[2]. Over 80 000 tonnes of antifouling paint which cost about € 1 billion are used every year in order to prevent fouling. The US Navy faces annual costs from fouling of over € 1 billion.

Increased fuel consumption leads to more pollution to the environment. For instance, the emissions of carbon dioxide, nitrogen oxides, sulphur oxide, hydrocarbons and particles increase. In addition, toxic antifouling agents or biocides in the antifouling paints have adverse effects on the marine ecosystems, which is needed to be considered as well ^[2].

The use of toxic antifoulants on ship hulls has been a historic method of controlling fouling but biocides such as lead, arsenic, mercury and their organic derivatives have been banned due to the environment risks that they posed ^[3]. The most famous and successful one was the SPC-TBT coating (Self Polishing Coating – Tributyltin) due to its great efficiency and versatility. The release rate can be controlled so that the lifetime is long. However it was eventually banned due to the severe effect on the environment ^[4]. Since the phasing out of TBT in 2001, alternatives have been available including biocide-free antifouling coatings and also tin-free SPC paints, but they are not

as effective as TBT. Therefore, booster biocides are incorporated in order to maintain the efficiency of the antifouling coating systems. But there have been severe issues concerning the persistence of the paint because of the premature leakage of the booster biocides. As a result, the cost of alternatives can be double in relation to the TBT-based paints (lifetime is 4-5 years ^[5]) due to the short lifetime of these alternative technologies ^[3, 6].

To prolong the lifetime of the coatings, microencapsulation which encapsulates the biocides in to form a core-shell structure, so called microcapsules, is a robust and promising tool to protect the biocides as well as control and extend its release ^[7, 8]. There's technical difficulty in stabilizing the microcapsule suspensions due to their poor colloidal stability. Excess dispersant is needed in the suspensions to prevent aggregations of microcapsules. Another problem of this method is that the diffusion of biocides through the shell is too fast. Since the shell is made of hydrophobic polymer, and the biocides are typically hydrophobic as well, therefore the shell of the microcapsules is a poor barrier to prevent the premature release.

The two specific aims of this master project are, first to increase the colloidal stability of microcapsule system, and second to reduce the release rate of biocides from microcapsules.

The colloidal stability can be increased by the use of charged microcapsules. The high surface charge on the microcapsules will increase the colloidal stability based on the electrostatic stabilization. The release rate can be controlled by creating a hydrophilic barrier on the surface of microcapsules against the typically hydrophobic biocides. This may be achieved using the charged microcapsules as templates for Layer-by-Layer (LbL) assembly of polyelectrolytes. Another possible modification is to use charged liposomes to build lipid bilayers on the surface of microcapsules. Below the phase transition temperature (T_c) of the lipid, the bilayer is frozen in a tightly packed crystalline structure which can be a very firm barrier against any active substance.

Theory

Microencapsulation

Microencapsulation is a process of enclosing a substance inside a miniature capsule. Tiny droplets, or particles of liquid or solid material, are packed within a second material or coated with a continuous film or polymeric material^[9]. The material that is coated or entrapped is most often a liquid but could also be a solid or gas and is referred to as the core materials, or internal phase. The material that forms the coating is referred to as the wall materials, shell or simply coating^[10]. The product obtained by microencapsulation is a sphere which has a diameter between a few micrometers and a few millimeters with a uniform wall around it. The microparticles are called microcapsules or microspheres depending on the morphology and internal structure. The microcapsule is a core-shell system, while the microspheres are homogeneous spherical particles. The size of the capsules plays a very important role for controlled release applications^[11]. A large total surface area is obtained due to the microscopic size of microcapsules, which is the most significant feature with respect to adsorption/desorption, chemical reactions, etc.

The microcapsules used throughout this work are systems with a polymer as the shell and alkane oil as the core in which an active substance can be dissolved.

Microencapsulation techniques

Microcapsules can be prepared by various techniques, many of which are modifications of the three basic techniques: spray-drying, phase separation (coacervation), and solvent evaporation/extraction^[17].

Relatively, spray drying is the most common and simple but still the most economical and widely used method of microencapsulation. Figure 2 shows the schematic illustrating of the microencapsulation process by spray drying. When preparing materials for spray drying, the wall material is hydrated. The substance to be encapsulated is added to the wall material and mixed thoroughly by homogenizing or other similar techniques to create an emulsion. Then the mixture is fed into a spray dryer where it will be atomized through a nozzle. Hot air flowing in either a co-current or counter-current direction contacts the atomized particles and evaporates the water, producing a dried particle with small droplets of core contained in the wall material. The dried particles then fall to the bottom of the dryer and are collected^[9].

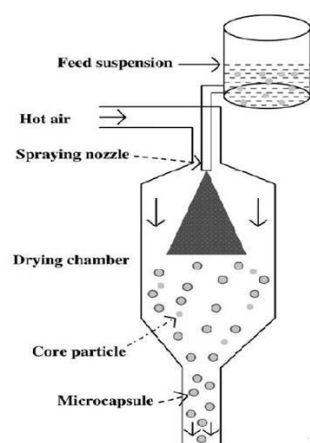


Figure 2. Schematic illustrating the process of microencapsulation by spray drying.

Spray drying requests lower processing costs, readily available equipment, and is of high throughput. However, the powder it produces needs to be further processed if it is for a liquid application, also the required heat for evaporation of water from the system makes spray drying not a good technique for highly temperature-sensitive compounds ^[9, 10].

For the phase separation, the first systematic approach of it was realized by Bungenberg and colleagues ^[18], which was the first reported process to be adapted for the industrial production of microcapsules.

Currently, phase separation processes are simply divided into two methods, simple and complex coacervation. The mechanism of microcapsule formation for both processes is identical, except for the way in which the phase separation is carried out. In simple coacervation, a desolvation agent is added for phase separation, whereas complex coacervation involves complexation between two oppositely charged polymers ^[12].

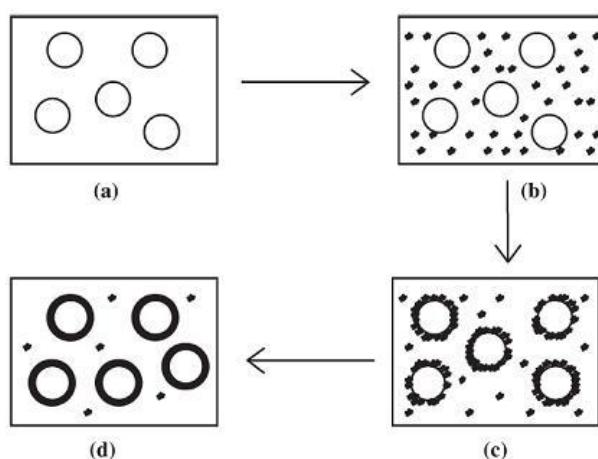


Figure 3. Schematic representation of the coacervation process. (a) Core material dispersion in solution of shell polymer; (b) Separation of coacervate from solution; (c) Coating of core material by microdroplets of coacervate; (d) Coalescence of coacervate to form continuous shell around core particles.

Figure 3 shows the schematic representation of the coacervation process. Microencapsulation by

coacervation is carried out by preparing an aqueous polymer solution at a proper high temperature into which the core material (hydrophobic) is also dispersed. A suitable stabilizer may also be added to the mixture to maintain the individuality of the final microcapsules. A suitable coacervating agent is gradually introduced to the mixture, which leads to the formation of partially desolvated polymer molecules, and hence their precipitation on the surface of the core particles. Then the coacervation mixture is cooled down, followed by the addition of a crosslinking agent to harden the microcapsules wall formed around the particles ^[12].

Solvent evaporation

Solvent evaporation/extraction has been used by many companies, including the NCR company, Gavaert Photo – Production NV, and Fuji Photo Film Co., Ltd, etc ^[9]. The polymer is dissolved in a water immiscible volatile organic solvent, like DCM or chloroform, into which the core material (e.g. oil and active substances) can also be dissolved or dispersed. The resulting solution, the oil phase, is added dropwise to an aqueous solution having a suitable stabilizer (such as poly(vinyl alcohol), abbreviated PVA), under vigorously stirring using a high-shear homogenizer, to form small polymer droplets containing the encapsulated material. With time, the microcapsules are produced by the removal of the solvent from the polymer droplets either by solvent evaporation or by solvent extraction (with a third liquid which is a precipitant for the polymer and miscible with both water and solvent). Solvent extraction produces microcapsules with higher porosities than those obtained by solvent evaporation ^[12].

When making microspheres, the only difference through the whole procedure is to prepare the oil phase without adding dodecane. The basis of this method is shown schematically in Figure 4.

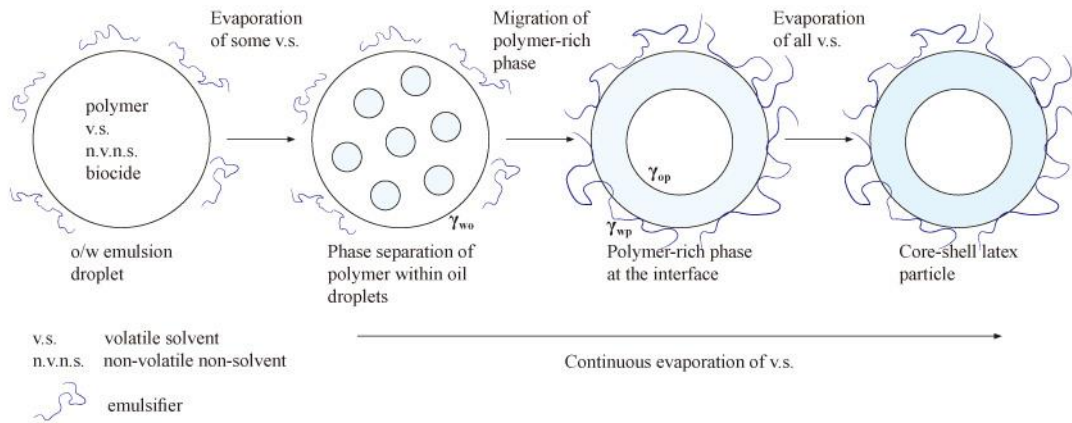


Figure 4. Schematic representation of the mechanism of microencapsulation based on solvent evaporation; v.s. = volatile solvent; n.v.n.s. = non-volatile non-solvent;

Different morphologies when mixing the droplets of immiscible liquids (phases 1 and 3) with a third mutually immiscible liquid (phase 2) was studied by Torza and Mason ^[15]. By analyzing the various interfacial tensions between the phases (γ_{12} , γ_{23} and γ_{13}), the final equilibrium morphology could be rationalized. The spreading coefficients for each phase was defined as

$$S_i = \gamma_{jk} - (\gamma_{ij} + \gamma_{ik}) \quad (1)$$

and designating phase 1 to be that for which $\gamma_{12} > \gamma_{23}$, then $S_1 < 0$. Then there are three possible combinations of S_i ,

$$S_1 < 0; \quad S_2 < 0; \quad S_3 > 0, \quad (2)$$

$$S_1 < 0; \quad S_2 < 0; \quad S_3 < 0, \quad (3)$$

$$S_1 < 0; \quad S_2 > 0; \quad S_3 < 0. \quad (4)$$

When the conditions in Eq. (2) are satisfied, a core-shell morphology (Figure 5a) is formed, with phase 1 appearing as the core within a shell of phase 3. When Eq. (3) is satisfied, “acorn”-shaped particles (Figure 5c) are formed, and when Eq. (4) is satisfied, two separate droplets are preserved ^[15].

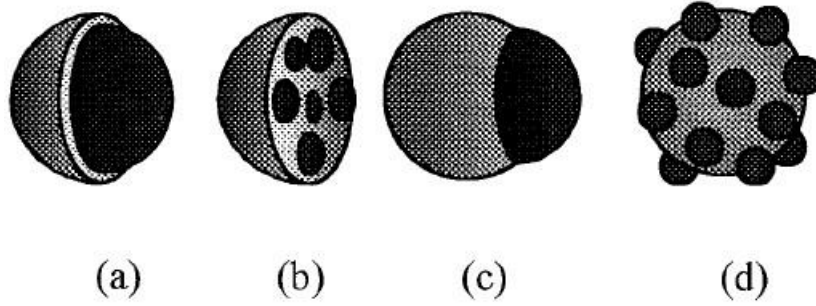


Figure 5. Four possible two-phase morphologies: (a) core/shell, (b) occluded, (c) “acorn”, and (d) heteroaggregate ^[15].

In this work, phase 1 is oil, phase 2 is water, and phase 3 is polymer. Even though one phase (the shell polymer) is solid, the above analysis is still valid since on phase separation the polymer phase is a solvent-rich liquid. For the microencapsulation to be successful, the polymer must spread between the oil and water phase to form a core-shell system, which means that the spreading condition, $S_P = \gamma_{WO} - (\gamma_{WP} + \gamma_{OP}) > 0$, must be fulfilled. This requires that the emulsifier is not too surface active since this will reduce the γ_{WO} interfacial tension and hence disable core-shell formation.

Size of the microcapsules

The size of the microcapsules is determined by several factors, such as emulsifiers, viscosity, shear rate, etc. The type of emulsifier is one of the most important ones. A more surface active emulsifier will result in a lower oil-water interfacial tension, hence the droplet size will be smaller ^[41].

Furthermore, the addition of a water soluble co-solvent, like acetone, to an oil phase results in smaller droplets when this solution is emulsified. Since acetone is more hydrophobic than water and less hydrophobic than the good solvent (which is DCM in this work), it will be distributed between the phases, and therefore reduce the interfacial tension. This is the reason why addition of

co-solvent acetone leads to smaller size droplet ^[41, 42].

Another significant factor affecting the droplet size and consequently the microcapsule size is the shear rate, i.e. stirring, during the emulsification. A higher shear rate will form smaller droplets due to the higher energy provided to the whole system ^[41].

Viscosity affects the droplet size as well. A higher viscosity will form bigger droplets, because the system requires more energy to agitate ^[40].

In addition to the above factors, altering the concentration of shell forming polymer and the volume of the aqueous phase may change the size of the particles as well. Different concentrations of shell material will lead to shells of different thickness and therefore form droplets of different sizes ^[40].

Layer-by-Layer Techniques

The stepwise polyelectrolyte assembly on the surface of the particles using the well-known layer-by-layer (LbL) technique ^[25] is of considerable interest because of its wide spectrum of potential applications such as corrosion control, biomedical applications ^[17], construction of semiconductor nanoparticles materials ^[16], and release control ^[43], etc. This method is performed by consecutively adsorbing oppositely charged polyelectrolytes on to a charged template, which can be either a macroscopic planar surface or the surface of a colloid ^[26]. The process is shown in Figure 6. The driving force is mainly the strong electrostatic interaction between oppositely charged species (e.g. polyelectrolytes, DNA, proteins or even colloids) ^[17].

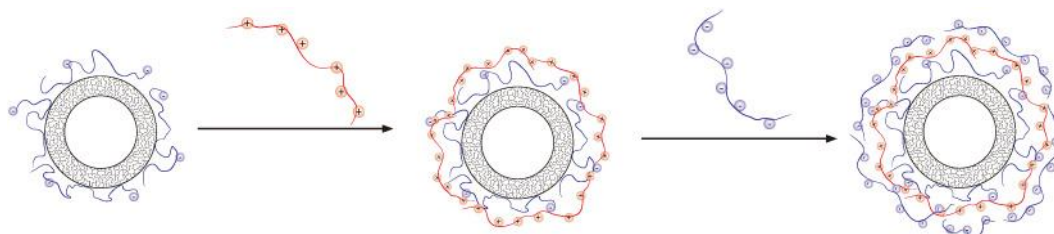


Figure 6. Schema of stepwise LbL assembly on a charged template.

Since the technique allows interfacing a wide variety of materials, it has been successfully introduced to both material science and applied biosciences ^[17]. LbL is a perfect method in controlling thickness, which is due to the linear growth of the films with the number of layers. However, a challenge for the LbL technique is to increase the process rate in order to adapt to the requirements of modern industry.

In order to build polyelectrolyte layers on the surface of microcapsules, a highly charged surface is required since the electrostatic interaction is the dominant driving force for adsorption. Apart from this, the Van der Waals force, which is the sum of the attractive or repulsive forces between molecules (or between parts of the same molecules), has an effect on the adsorption of polyelectrolytes as well ^[47].

Salt also plays an important role during the adsorption. When the salt concentration is low or there's no salt in the system, the polyelectrolyte adsorbed on the surface of microcapsules is flat (see Figure 7), resulting in an almost neutral surface after the adsorption of polyelectrolytes. When the salt concentration is high enough, the polyelectrolytes will be adsorbed on the surface as a coil, occupying less space for each molecule, therefore there will be more polyelectrolytes adsorbed, and the compensation of charges on the surface can be achieved ^[47].

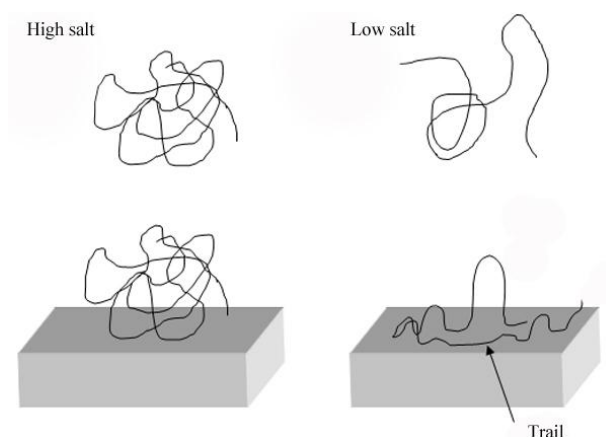


Figure 7. The effect of salt concentration on adsorption of polyelectrolytes.

Liposomes and lipid bilayers

Lipids are a type of surfactants consisting of a polar head group and two hydrophobic tails, usually of the same size. The packing parameter is therefore approximately one and the lipids therefore preferably form lamellar structures in solution ^[44]. Liposomes, or lipid vesicles, are colloidal particles of dispersed lamellar phases consisting of one or more concentric bilayers of lipids encapsulating aqueous space or spaces ^[27] (see Figure 8). It was not until in 1962 when Alec D. Bangham and his colleague, R. W. Horne examined phospholipid dispersions in water by negative staining using sodium phosphotungstate and ammonium molybdate and obtained conclusive experimental evidence that phospholipids could self-assemble to form 'bag-like' structures which their colleague Gerald Weissman named liposomes ^[27-29]. There are a lot of applications of liposomes, such as the delivery of enzymes ^[30] or anticancer drugs ^[31], cosmetic agents for the delivery of moisturizers ^[32], carriers of drugs, etc.

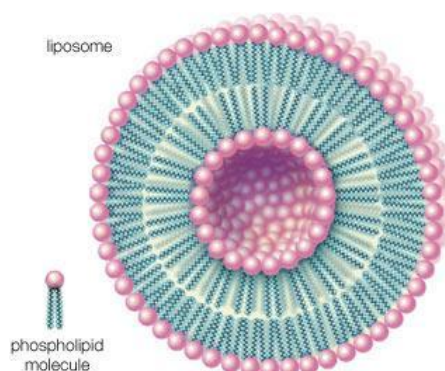


Figure 8. The structure of liposomes ^[45].

At a New York Academy of Sciences meeting reported in 1978 ^[33], liposomes were classified by several three letter acronyms as follows: multilamellar vesicles (MLV), small unilamellar vesicles (SUV), and large unilamellar vesicles (LUV).

Liposomes must be prepared at temperatures above the chain-melting temperature (T_c) of the lipid so that the bilayers are in the liquid-crystalline state ^[27]. The chain-melting temperature of a lipid increases with the alkyl chain length, decreases with the amount of unsaturations and depends also on the head group type ^[34]. Generally, the permeability rate of liposomes increases with increasing temperature, with an abrupt large increase at T_c ^[35]. Below T_c , the bilayers are in a non-permeable state, which is why we believe that lipid bilayers are good barriers for controlling the release rate of actives.

The general elements of the procedure of liposome formation involve preparation of the thin lipid films for hydration, hydration with agitation, and sizing to a homogeneous distribution of vesicles. The mechanism of liposome formation is shown in Figure 9. The same preparation method can be used for all lipid vesicles regardless of composition. Mean size and distribution of liposome is influenced by composition and concentration, temperature, sonication time and power, volume, etc ^[23].

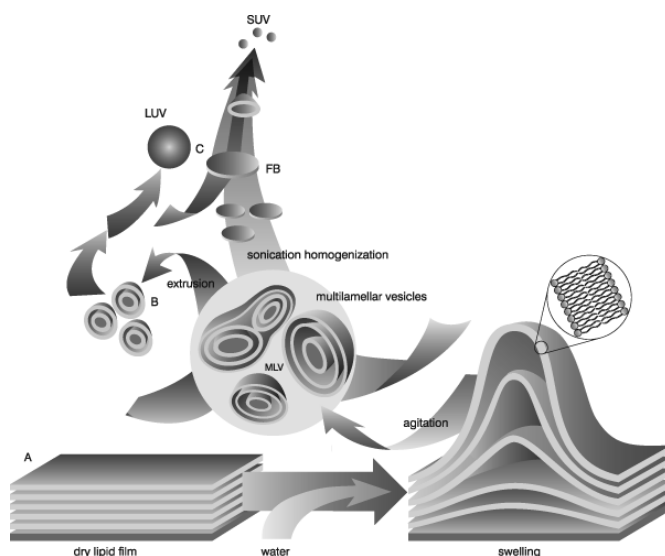


Figure 9. Mechanism of liposome formation ^[23].

The structure of the particle with charged lipid bilayers coated on the oppositely charged particles adsorbed with PEs multilayers is shown in Figure 10. It is believed that the SUVs will first be adsorbed on the surface of microcapsules, then deformed by the electrostatic interaction, and finally ruptured to form lipid bilayers. The driving force for both rupture and adsorption is the electrostatic interaction between the charged lipids and the surface of microcapsules. When the electrostatic interaction is not large enough to rupture the vesicles into lipid bilayers, then the lipid vesicles will be directly adsorbed on the surface ^[48].

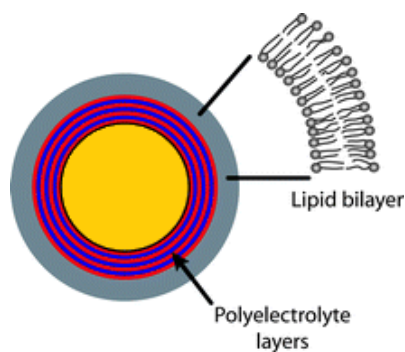


Figure 10. The structure of lipid bilayers coated on the PEs multilayer particles.

Experimental

Light Microscopy

Light microscopy (or optical microscopy) has a wide variety of applications. It is a very powerful tool for investigating the microstructure of a great range of materials. It involves passing visible light transmitted through or reflected from the sample through a single or multiple lenses to allow a magnified view of the sample. The resulting image can be detected directly by the eye. Lenses, oculars, light source, camera, sample stage and support, make up the basic light microscope ^[37].

There are two modes to inspect the sample, reflected-light mode and transmission mode. Reflected-light microscopy is used for a range of materials, including metals, ceramics and composites. Transmission mode can be used when the sample is transparent ^[37].

Dark field microscopy

Darkfield microscopy is a specialized illumination technique to enhance the contrast in samples that are not imaged well under normal brightfield illumination conditions ^[18]. It works by illuminating the sample with the light that will not be collected by the objective lens, and thus will not form part of the image. This produces an image of a dark, almost black, background with bright objects on it ^[19].

The steps are illustrated in Figure 11.

- (1) Light enters the microscope from a light source.
- (2) An opaque disc (dark field patch stop) is placed below the condenser lens which focuses the light towards the sample.
- (3) The light enters the sample. Most light is directly transmitted, while some is scattered from the sample.
- (4) Only the scattered light enters the objective lens and produces the image. The directly transmitted light is blocked by a direct illumination block ^[19].

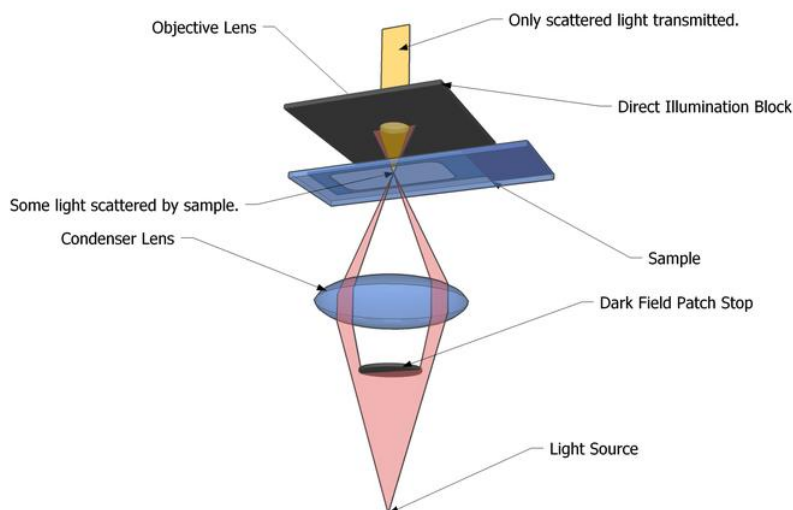


Figure 11. Diagram illustrating the light path through a dark field microscope ^[19].

Darkfield microscopy is a low-cost and very effective technique with simple setup. It's ideal for viewing objects that are unstained, transparent and absorb little or no light ^[20]. However, this technique also comes with a number of disadvantages. For example, low contrast levels seen in the final image require the use of extremely strong illumination, which can damage the sample.

Microelectrophoresis

Microelectrophoresis is a method of studying electrophoresis of various dispersed particles using optical microscopy. This method provides an image of moving particles, which is its unique advantage.

Experimental considerations

During microelectrophoresis, two important experimental conditions need to be fulfilled. First, the concentration of the sample must be sufficiently low for observing individual particles, which means diluting sample is necessary before the measurements. Second, the electro-osmosis generated by electric field will influence on the double layers of the sample cell walls. The walls of the electrophoresis cells will normally be charged in the presence of a solvent (usually negatively in water). The charge leads to the electro-osmotic flowing of the oppositely charged solvent towards the corresponding electrode. The velocity of this flow varies across the cell due to the reversed laminar flow caused by the pressure difference between the two ends. The combination of these two opposing flows leads to the situation where the solvent is stationary only in clearly defined areas of the cell: *the stationary levels* (see Figure 12). The stationary level, i.e. where the solvent is stationary, is thus the only place possible to measure the electrophoretic velocity of any particles in the sample. So the microscope needs to be focused on this stationary layer before each measurement so that particles motion will not be affected by electro-osmosis when observing ^[21].

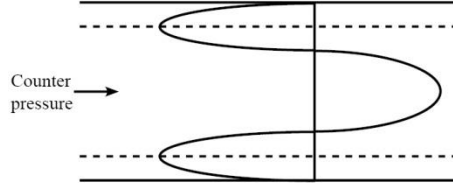


Figure 12. The flow velocities in a capillary cell for ζ measurements.

The electric double-layer and electrophoresis

When a charged object is in contact with an aqueous solution, an electric double-layer will form (Figure 13). The first layer consists of condensed counterions. The second layer, or the diffuse layer, is composed of free ions which move in the fluid under the influence of electrostatic interaction and thermal motion ^[38].

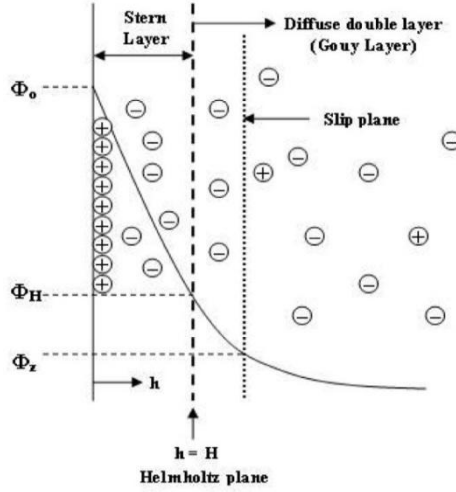


Figure 13. Schematic diagram of an electric double layer.

In the case of low Reynolds number and moderate electric field strength E (V/l , where V is the voltage and l is the effective inter-electrode distance), the velocity of a dispersed particle v is simply proportional to the applied field, which leaves the electrophoretic mobility μ_e defined as ^[26]:

$$\mu_e = \frac{v}{E} \quad (5)$$

The equation (7) converting mobility to effective electro-kinetic potential (ζ) depends on the value of the dimensionless quantity κa in which a is the radius of the particle (assumed spherical) and κ , the Debye length, is the quantity:

$$\kappa^2 = \frac{e^2 \sum n z^2}{\epsilon K T} \quad (6)$$

The electrophoretic mobility μ_e was then converted to the ζ -potential using the Smoluchowski relation, according to,

$$\mu_e = \frac{\varepsilon \varepsilon_0 \zeta}{\eta} \quad (7)$$

where, ε is the dielectric constant of water, ε_0 is the permittivity of free space, ζ is the zeta potential of the particles, and η is dynamic viscosity of water.

Smoluchowski is valid only for sufficiently thin double layer, when particle radius a is much greater than the Debye length κ^{-1} which is valid for our microparticles:

$$a\kappa > 100 \quad (8)$$

When Debye length is larger than particle radius:

$$a\kappa < 1 \quad (9)$$

The Hückle equation (10) should be used to calculate the electrophoretic mobility μ_e :

$$\mu_e = \frac{2\varepsilon \varepsilon_0 \zeta}{3\eta} \quad (10)$$

ESCA

ESCA (Electron Spectroscopy for Chemical Analysis), which is also known as XPS (X-ray photoelectron spectroscopy), is a surface sensitive technique used to determine atomic compositions and to extract information about different types of bonding in the sample. Different chemical environment around an atom of interest influences the electronic environment creating a “chemical shift” which acts as part of the compound’s fingerprint. For instance, a carbon of a carboxyl group will behave slightly different than that of a carbon in a methyl group ^[22].

The samples are usually solid because ESCA requires ultra-high vacuum. The sample is irradiated with a focused beam of X-rays, which causes electrons from the very top surface (1-4nm) of the sample to be photo-emitted. The escaped electrons are collected with an electron collection lens. The kinetic energy and number of electrons are measured simultaneously and the XPS spectra are obtained ^[22].

SEM

SEM (Scanning Electron Microscopy), is a type of electron microscope that images a sample by scanning across the surface with a high-energy electron beam. The impact of the beam with the surface generates a cascade of electrons that are scattered in all directions. The amount of electrons generated at the surface, and their energy, depend on the topography and the elements that the analyzed material consists of. Thus, both topographic and elemental information can be obtained. Since electrons have much higher energy than photons, they also have much smaller wavelengths. The resolution can therefore be drastically improved compared to that of an optical microscope ^[39].

Material and Methods

Material

All the chemicals, acetone (99.8%), Dichloromethane ($\geq 99.5\%$), Poly(methyl methacrylate) (PMMA, $M_w=350k$), sodium chloride were purchased from Sigma-Aldrich. Dodecane (99%) and Poly(vinyl alcohol) (95%, $M_w=95k$) were purchased from Fisher Scientific. Milli-Q water (resistivity 18.2 M Ω cm) was provided by a Millipore “Milli-Q plus” unit.

Emulsifier

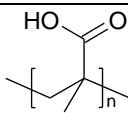
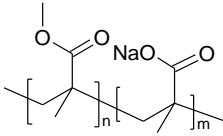
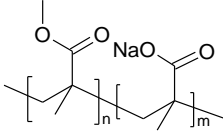
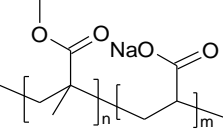
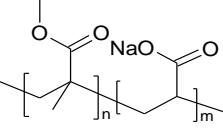
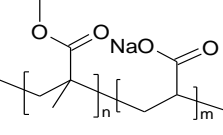
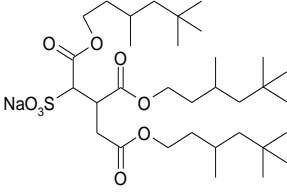
In this project, three methods using ionic emulsifiers were used to synthesize charged microcapsules. The first method was using the conventional emulsifier Poly (methacrylic acid) (PMAA, $M_w=100k$) (Polysciences, Inc.), a weak polyelectrolyte, to form the negatively charged template microcapsules [15].

The second method was using amphiphilic block copolymers (Polymer Source, Inc.), consisting of one hydrophobic PMMA block and a hydrophilic PMANa or PANa polyelectrolyte block. We believed that the hydrophobic PMMA block may anchor the hydrophilic polyelectrolyte block on the capsule, providing the particles with a high charge.

The third method was using the hydrophobic anionic surfactant TC4 (Sodium, 5-dioxo-1, 5-bis (3, 5, 5-trimethylhexyloxy)-3- ((3, 5, 5-trimethylhexyloxy) carbonyl) pentane-2-sulfonate) (as kindly provided by Julian Eastoe [24]) in the oil phase and the polycation, PDADMAC, in the aqueous phase in order to produce positively charged microcapsules. PDADMAC was believed to be able to absorb with the aid of the anionic surfactant TC4, providing the capsule with a high positive surface charge.

The structures and the molecular weight of all the emulsifiers are listed in Table 1.

Table 1. The structures and molecular weight of the emulsifiers.

Name	Structure	M _w
Poly(methacrylic acid), PMAA		100000
Poly(methyl methacrylate-b-sodiummethacrylate)		PMMA(600)-b-PMAANa(4600)
Poly(methyl methacrylate-b-sodiummethacrylate)		PMMA(4000)-b-PMAANa(9300)
Poly(methyl methacrylate-b-sodium acrylate)		PMMA(4300)-b-PAANa(17500)
Poly(methyl methacrylate-b-sodium acrylate)		PMMA(5500)-b-PAANa(6200)
Poly(methyl methacrylate-b-sodium acrylate)		PMMA(18000)-b-PAANa(57400)
Sodium 1,5-dioxo-1,5-bis(3,5,5-trimethylhexyloxy)-3-((3,5,5-trimethylhexyloxy)carbonyl)pentane-2-sulfonate, TC4		624

Polyelectrolytes

Two kinds of polyelectrolytes were used during the LbL assembly, poly (diallyldimethyl ammonium chloride) (PDADMAC, 40 wt% in water) (as kindly provided by Michael Persson, Akzo Nobel), and PMAANa (30 wt% in water, Mw=15000) (Sigma-Aldrich). The structures are shown in Figure 14.

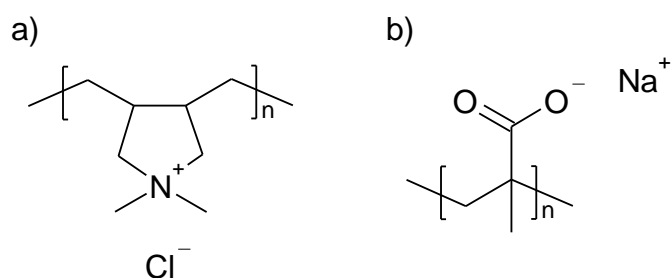


Figure 14. The structures of the polyelectrolytes. a) PDADMAC; b) PMAA Na.

Lipids

In this work, two kinds of lipids were used, the cationic DA (H) (di(hydrogenated tallow) alkyl dimethyl ammonium chloride) (as kindly provided by Christy Whiddon, Akzo Nobel), and the anionic DSPA (1, 2-di-octadecanoyl-*sn*-glycero-3-phosphate (sodium salt)) (Avanti Polar Lipids, Inc.). The structures are shown in Figure 15.

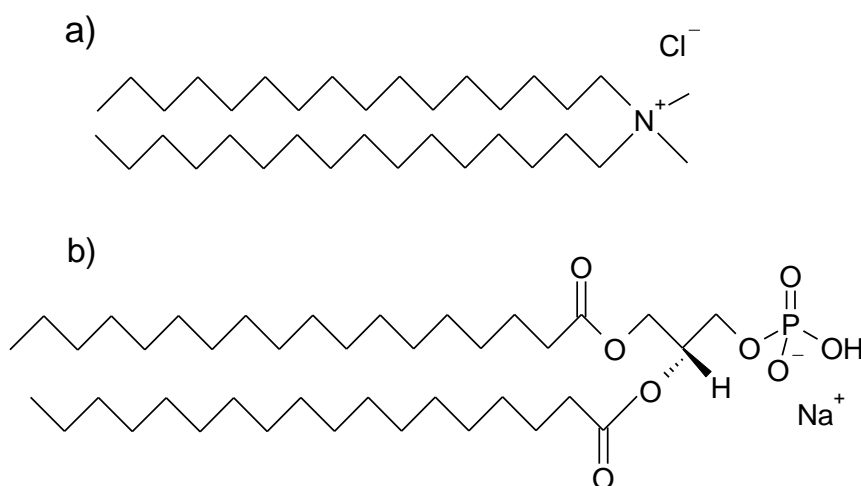


Figure 15. The structures of the lipids. a) DA(H), b) DSPA.

Methods

Preparation of microcapsules and microspheres

Both microcapsules and microspheres were prepared with the solvent evaporation technique^[19] as previously described in theory session, using a motor (Heidolph Silent Crusher M) and a high shear homogenizer (Heidolph TYP 22 F/M). The oil phase and the aqueous phase were prepared separately. The emulsifier was dissolved in Milli-Q water (with the exception of TC4 which was dissolved in the oil phase) at elevated temperature under vigorously stirring. For microcapsules, PMMA was dissolved in the oil phase (a mixture of DCM, acetone, and oil) at room temperature. For microspheres, double amount of PMMA compared to that of microcapsules was dissolved in the oil phase which was a mixture of only DCM and acetone.

The aqueous phase (40 vol% of the solution, 80ml of a 200ml aqueous phase) was homogenized in

a three-necked flask at 5000rpm during the dropwise addition of the oil phase. The stirring was raised to 10000rpm, or 7500rpm, for one hour during the emulsification. The emulsion was then immediately poured into the remaining aqueous phase and placed in a fume hood under vigorously stirring. The dispersion was left overnight for evaporation of DCM and acetone, with subsequent formation of microcapsules or microspheres.

Summary of all microencapsulations

In the experiments, 200ml and 50ml batches (the volume of aqueous phase) were used to synthesize microcapsules. The concentration of PMMA in the oil phase was 2.000 wt%. The concentration of the emulsifier was either 1.275 wt% or 0.400 wt% in the aqueous phase, with the exception of the block copolymer PMMA(18000)-b-PANa(57400), where a concentration of 0.050 wt% was used due to the high viscosity when it was dissolved in the water. Regarding capsules prepared using TC4 and PDADMAC as emulsifiers, the concentration of TC4 in the oil phase was 0.050 wt%, 0.0125 wt% and 0.005 wt%. The shear rate was set to 10000rpm or 7500rpm according to the requirement of the capsules' size. All the syntheses are listed in Appendix I.

Polyelectrolyte Layer-by-Layer Adsorption

In this work, polyelectrolyte multilayer assembly was accomplished by the consecutive adsorption of oppositely charged polyelectrolytes (PEs) with one intermediate washing step including centrifugation (Avanti J-20xp, Beckman Coulter, Inc.) of the crude suspension followed by redispersing the precipitate in Milli-Q water. The purpose of the washing step is to discard the free PEs in the suspension.

PDADMAC and PMAA Na⁺ (30 wt% in water) were used as the polycation and polyanion respectively. The concentration of PEs was 1.0 wt% and the concentration of NaCl of PEs solution was adjusted to 2M or 1M to make a final concentration 1M or 0.5M after mixing with the microparticles of the same volume. In each experiment, the suspension of microparticles was added into the same volume of PE solution slowly (droplet by droplet) and mixed for around 5min under stirring. One washing step with water was carried out between two adsorption cycles. Sonication was used after each centrifugation to redisperse the suspension if necessary. LbL assembly was performed on all three types of charged capsules.

Lipid bilayer formation on charged particles

Preparation of small unilamellar vesicles (SUVs)

0.05g DA (H) was dissolved in 2ml chloroform in a pear shaped flask. The flask was then placed on a rotary evaporator for about 3 hours to remove all the organic solvent and obtain a dry thin lipid film. Large multilamellar vesicles (LMV) were generated by hydrating the lipid film by adding 5ml MQ water into the flask. The LMV were ultrasonicated in a bath for 1h at a temperature of 60 °C. The resulting suspension was extruded 11 times through a 100nm pore diameter polycarbonate filter at 60 °C to obtain the final lipid SUV suspension.

The same procedure was performed when preparing SUVs with DPPA. The amount of DSPA dissolved in the chloroform was 0.025g. The temperature during the rotary evaporation, sonication and extrusion was 78-80 °C due to the high transition temperature (75 °C) of DSPA.

Liposome adsorption, rupture and spreading on charged particles

A multilayer microcapsule solution with the outmost layer negatively or positively charged (depending on the charges of lipids) was added dropwise into the lipid SUV suspension under stirring (for around 20min).

When microcapsules with TC4 and PDADMAC as the emulsifiers were used as templates, the lipid bilayer assembly was performed directly on the charged particles without any LbL pretreatment, since we believe that the surface of this kind microcapsules is rather flat (see Figure 16 left), enabling more adsorption of lipid bilayers. Regarding the microparticles prepared using block copolymer as the emulsifier, the emulsifiers were most likely stretched out into the outside solutions (see Figure 16 right). Therefore, multilayers of polyelectrolytes (at least one layer) are adsorbed on the surface before adsorbing lipid bilayers.

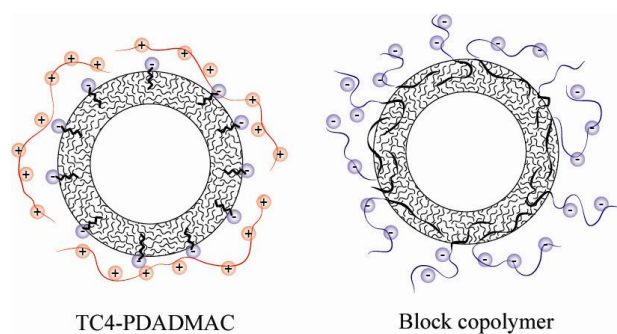


Figure 16. The structure of microcapsules synthesized with different types of emulsifiers.

Characterization

Light microscopy

In this work, optical microscopy was performed using an Olympus BH-2 light microscope equipped with a digital camera (Olympus DP1). $\times 50$ and $\times 100$ objective lenses were used to analyze the samples and to determine the size of microcapsules. The size and cumulative distribution of the microcapsules were obtained from a total of approximately 100 particles from the light microscopy images. The data were fitted according to a lognormal distribution function and also the corresponding cumulative distribution function using Matlab.

Microelectrophoresis

The ζ -potential of the colloidal particles was measured using a Micro-electrophoresis apparatus Mk II (Rank Brothers Ltd). The obtained electrophoretic mobility, u , was converted to the ζ -potential

using the Smoluchowski relation ($u = \epsilon \epsilon_0 \zeta / \eta$) as described in the theory section.

The sample was prepared by adding 10 μ l particle solution into 10ml 1mM NaCl solution. For each sample, 10 measurements were taken to obtain an average value. Also, between each measurement, the direction of the electric field was altered.

ESCA

The samples were analyzed on a Quantum 2000 Scanning ESCA Microprobe from Physical Electronics (a division of ULVAC-PHI).

Sample preparation

Microspheres (homogeneous PMMA particles) were prepared for ESCA measurements, since the vacuous conditions during the measurements may cause the oil to escape from the capsule and interfere with the instrument. For each sample, approximately 20 ml solution was taken, washed and dried.

PMAA as emulsifier and effect of pH

To study the effect of pH on the particles with the weak polyacid PMAA as emulsifier, microspheres were prepared according to the standard protocol as described in the methods section. Small volume of the microsphere suspension was taken out and centrifuged once to remove excess bulk emulsifier. The solid microspheres were redispersed in Milli-Q water and NaOH solution was added under vigorously stirring until the appropriate pH value was reached. The microsphere suspension of certain pH value was then centrifuged again and left to dry.

SEM

A LEO ULTRA 55 scanning electron microscope equipped with an Oxford Inca EDX system, a FEG gun (Field Emission Gun), an EBSD system and a STEM detector was used to investigate the final microcapsule morphologies.

The diluted sample of washed microcapsules was gold-coated in a sputter coater before being investigated under the scanning electron microscope.

Results and discussions

Characterization of microcapsules

Light microscopy and size distribution

As mentioned earlier, three types of microcapsules were synthesized in this work. Due to different chemical properties (charge, surface activity, etc.) of the emulsifiers, particles of different sizes were obtained (see Table 2). The results obtained using the three different kinds of emulsifiers are discussed below.

Table 2. The experimental data of successful batches.

Emulsifier	Volume of water/ml (batch size)	Wt% of emulsifier	Shear rate/rpm	Size/ μm
<i>Weak polyelectrolyte</i>				
PMAA	50	0.4000%	7500	3
<i>Amphiphilic diblock copolymers</i>				
PMMA(600)-b-PMANa(4600)	50	0.4000%	7500	1.5
PMMA(4300)-b-PANa(17500)	50	0.4000%	7500	<1
PMMA(4000)-b-PMANa(9300)	50	0.4000%	7500	5
PMMA(18000)-b-PANa(57400)	50	0.0500%	7500	5
<i>Hydrophobic anionic surfactant and polycation</i>				
TC4-PDADMAC	50	0.0125% ^a 0.1000% ^b	7500	2-3

^a Concentration of TC4 in the oil phase.

^b Concentration of PDADMAC in the water phase.

Weak polyelectrolyte

In Figure 17 and Figure 18, examples of light microscope photos and size distributions of capsules prepared using the conventional emulsifier PMAA are displayed. The capsules were prepared using two different batch volumes, also considered as the total volume of the emulsion; 50ml (a) and 100ml (b). The concentration of the emulsifier as well as the shear rate during the emulsification plays an important role with respect to the final size and size distribution of the capsules (see Table 1).

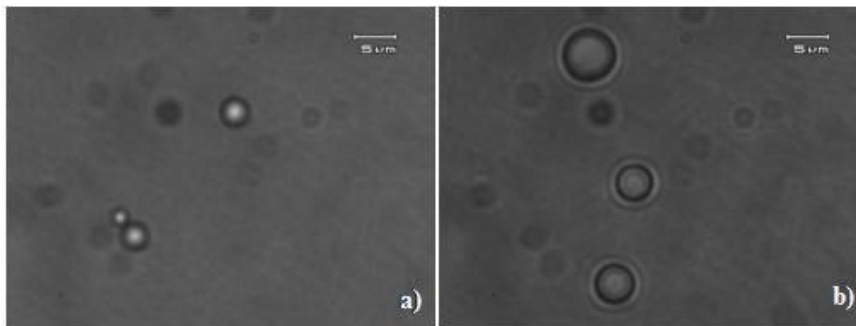


Figure 17. The light microscope photos of microcapsules prepared with PMAA as emulsifier and different conditions.

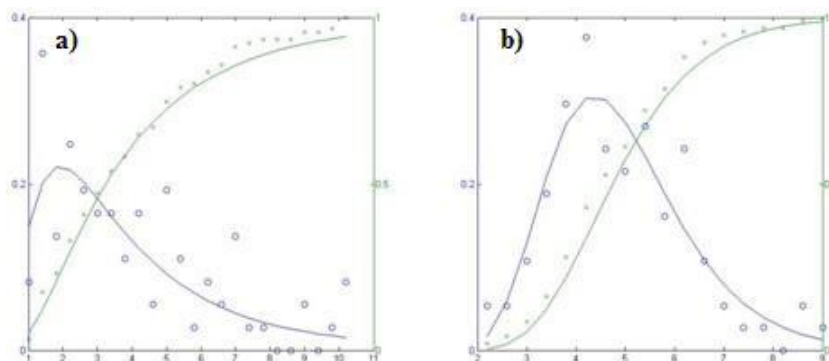


Figure 18. The size distributions of microcapsules prepared with PMAA as emulsifier and different conditions.

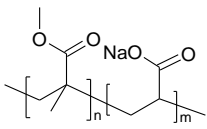
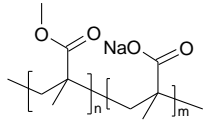
In Table 6 in Appendix II, it is shown that a change in the concentration of the emulsifier (1.2750% and 0.4000%) results in particles of slightly different sizes. Reducing the shear rate of the homogenizer (from 10000rpm to 7500rpm) results in larger particles, which is due to the fact that the higher energy (higher shear rate) provided by the homogenizer enables the formation of a larger surface area according to the equation $E = \gamma \cdot A$ (in this case, γ of two batches was the same). The difference in total volume of water can also alter the final size of the particles. Apparently, a smaller volume of 50ml will produce smaller particles, which might be the result of a more efficient mixing in the entire volume.

Amphiphilic diblock copolymers

A second type of microcapsules was successfully synthesized using different kinds of amphiphilic diblock copolymers as emulsifiers. The structures and the molecular weight of all the copolymers used in this work are shown in Table 3. The copolymers contain two parts, a hydrophobic PMMA block and a highly charged polyelectrolyte block.

Five copolymers with different lengths of the amphiphilic parts were used, four of which were successful to produce microcapsules. However, microcapsules formation using the copolymer, PMMA(5500)-b-PANa(6200), was unsuccessful. It was observed that solids were precipitating in the suspension during the emulsification. This might be resulted by the relatively high hydrophobicity of this copolymer, which made it hard for the copolymer to dissolve in the water phase.

Table 3. The structures and molecular weight of copolymers.

	PMMA(4300)-b-PANa(17500)
	PMMA(5500)-b-PANa(6200)
	PMMA(18000)-b-PANa(57400)
	PMMA(600)-b-PMANa(4600)
	PMMA(4000)-b-PMANa(9300)

A SEM image of microcapsule synthesized with PMMA(600)-b-PMANa(4600) as emulsifier is shown in Figure 19 and Figure 20, which proved that the particles are really core-shell structured microcapsules. Light microscope photos and size distributions of the successful block copolymer capsules are shown in Figure 21 and Figure 22, and the experimental data of all four batches are shown in Table 2.

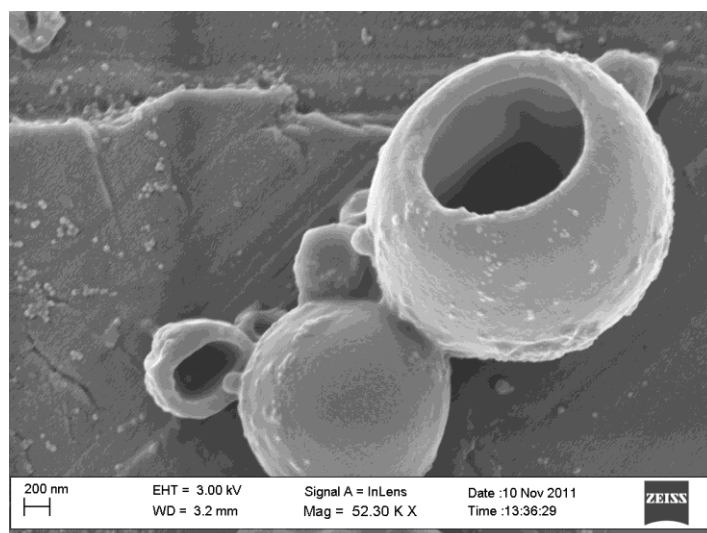


Figure 19. A SEM image of microcapsule (broken) synthesized with PMMA(600)-b-PMANa(4600) as emulsifier.

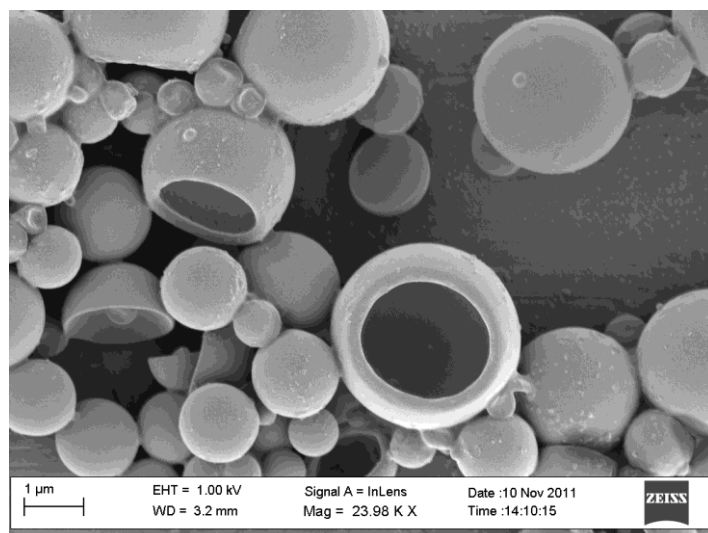


Figure 20. A SEM image of microcapsule synthesized with PMMA(600)-b-PMANa(4600) as emulsifier.

The dissolution of the copolymers was very slow, especially for PMMA(4300)-b-PANa(17500) and PMMA(4000)-b-PMANa(9300), even at high temperatures. After complete dissolution, the aqueous phase had a relatively high viscosity. This might be explained by the amphiphilic nature of the block copolymers. Similar to surfactants, amphiphilic block copolymers may self-assemble to a variety of structures. The CMC for these block copolymers are usually very low and the size of the individual micelles is rather large. At high concentrations, the micelles will overlap which significantly increases the viscosity of the solution. Encapsulation using PMMA(18000)-b-PANa(57400) as emulsifier at a concentration of 0.4000 wt% resulted in a gel-like aqueous phase. The concentration of this particular emulsifier was thus reduced to 0.0500 wt%. Because of the high molecular weight of this copolymer, larger micelles were formed which could overlap more compared to other copolymers, and therefore the viscosity was remarkably high.

Regarding the capsules prepared with PMMA(4300)-b-PANa(17500) as the emulsifier, the size of particles was too small that it was difficult for them to be seen clearly under the light microscope due to the limitation of its resolving power, and the size distribution was narrow.

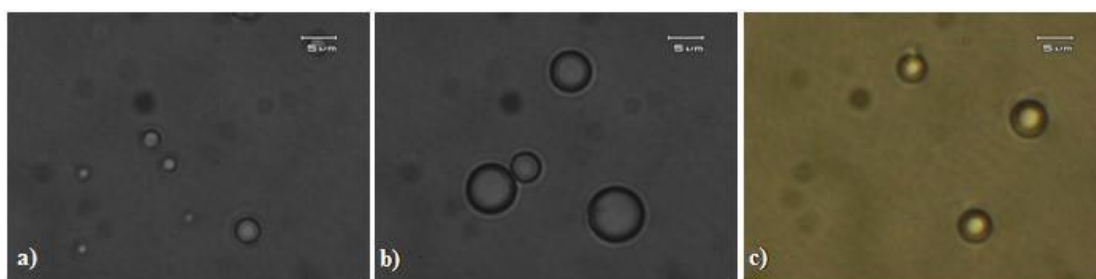


Figure 21. The light microscope photos of microcapsules prepared with different block copolymers as emulsifiers. a). PMMA(600)-b-PMANa(4600); b). PMMA(4000)-b-PMANa(9300); c). PMMA(18000)-b-PANa(57400).

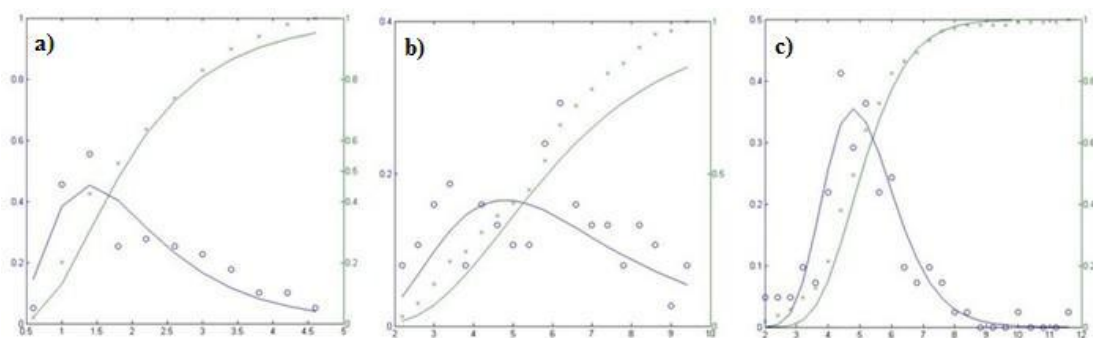


Figure 22. The size distributions of microcapsules prepared with different block copolymers as emulsifiers. a). PMMA(600)-b-PMANa(4600); b). PMMA(4000)-b-PMANa(9300); c). PMMA(18000)-b-PANa(57400).

No general trend is observed regarding the size of the microcapsule when comparing the block copolymers with the conventional PMAA emulsifier. For instance, using PMMA(600)-b-PMANa(4600) as emulsifier results in smaller capsules whereas the opposite holds if PMMA(18000)-b-PANa(57400) was used as emulsifier. A possible explanation for the smaller size for PMMA(600)-b-PMANa(4600) than for PMAA might be that PMMA(600)-b-PMANa(4600) is more surface active and therefore prone to produce smaller capsules. Using this assumption, the size of microcapsules prepared with PMMA(4000)-b-PMANa(9300) should be smaller than with PMMA(4300)-b-PANa(17500), which is a result of a relatively higher surface activity of PMMA(4000)-b-PMANa(9300). However, the results were opposite, probably due to other kinetic effects, such as heating rate ^[46]. The size of microcapsules using PMMA(18000)-b-PANa(57400) as emulsifier was large, probably due to the very high viscosity of aqueous phase, which required more energy to disrupt the droplets, and droplet break-up was hard in this case.

Hydrophobic anionic surfactant and polycation

A third type of microcapsules was synthesized using a hydrophobic oil-soluble anionic surfactant and a polycation in combination. Earlier experiments showed that using only PDADMAC as the emulsifier failed to produce microcapsules. PDADMAC is most likely too water soluble, preventing it from adsorbing on the oil droplets or the PMMA surface. Yet, with the aid of the anionic surfactant TC4, PDADMAC was able to adsorb on the surface.

However, in order to fulfill the spreading conditions, it is required that TC4 is hydrophobic enough so as to maintain a high oil-water interfacial tension.

The light microscope photo of capsules and size distribution is shown in Figure 23. The size of capsules was around 2-3 μm , and the size distribution was narrow.

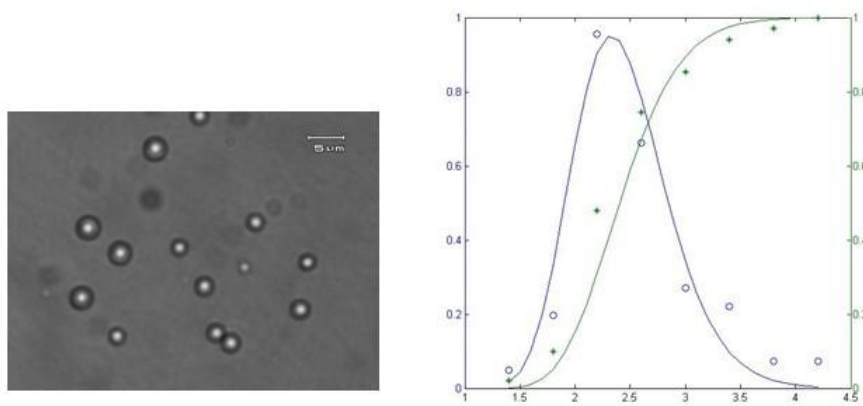


Figure 23. The light microscope photo and size distribution of TC4-PDADMAC capsules.

A SEM image of microcapsule synthesized with TC4-PDADMAC as emulsifier is shown in Figure 24. A FIB-SEM (Focused Ion Beam – SEM) image of this type microcapsule is shown in Figure 25. The microcapsules are perfectly spherical. Inside the microcapsule, there are small holes individual or connected with each other.

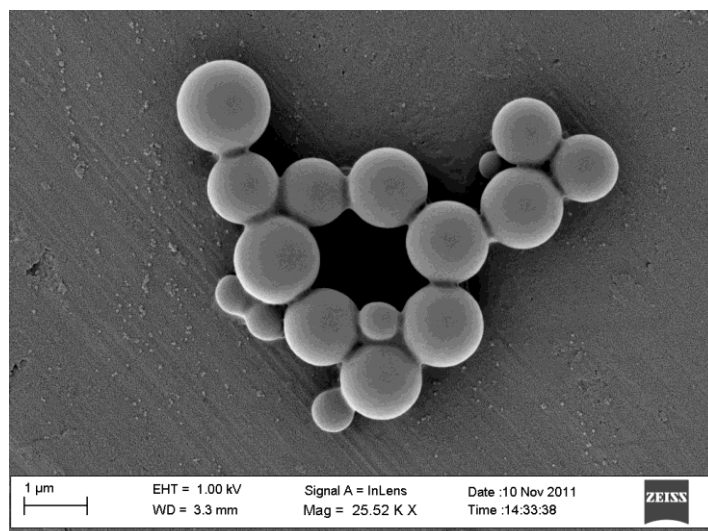


Figure 24. SEM image of microcapsules produced with TC4-PDADMAC as emulsifiers.

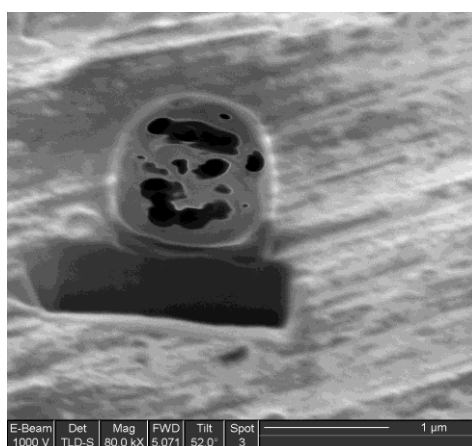


Figure 25. FIB-SEM image of microcapsules produced with TC4-PDADMAC as emulsifiers.

Microelectrophoresis and ζ -potential

Microelectrophoresis measurements were carried out for the initial (microcapsule or microsphere suspensions without any treatment) and redispersed (microcapsule or microsphere suspensions washed with MQ water) microparticle samples. The standard deviation was calculated for all the samples based on the raw data. The results of ζ -potential are displayed in Figure 26.

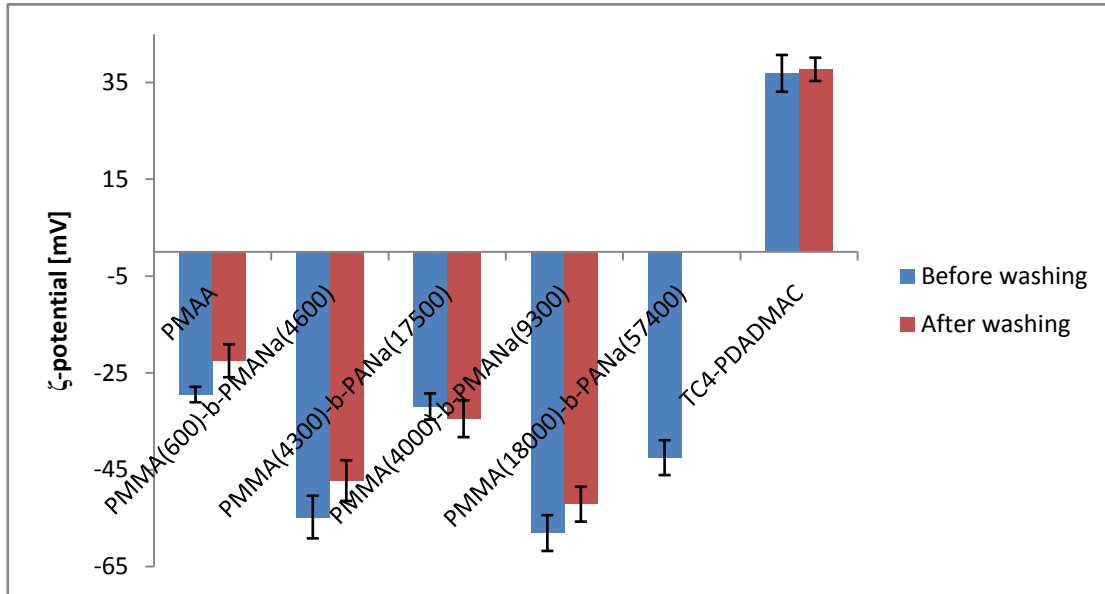


Figure 26. The ζ -potential values for all types of microcapsules both before and after washing.

Since PMAA is in its acid form, the ζ -potential is relatively low compared to the block copolymers. After washing with water, NaOH was added to adjust the pH value of the suspension to 7.0, so that the capsules could be redispersed. The introduction of charges increases the electrostatic repulsion between microcapsules and thereby the colloidal stability. However, after pH adjustments and washing steps, the ζ -potential was reduced to about -20mV. This is most likely due to some desorption of PMAA due to its increasing water solubility which is demonstrated below.

The capsules with block copolymers as the emulsifiers had a higher ζ -potential value. The high negative surface charges were mainly caused by the polyelectrolyte block of the block copolymers anchored strongly by the hydrophobic PMMA block on the capsule, so that even after washing, the value of ζ -potential was still high.

TC4-PDADMAC capsules demonstrated also a high ζ -potential value as well, however, the suspensions could only remain stable for 10 to 12 days, after which lots of solids precipitated. The reason might be that the hydrophobicity of TC4 was still not high enough to fulfill the spreading conditions.

ESCA results

PMAA as emulsifier and effect of pH

PMAA is a weak polyacid with a pKa of around 5.5 [36]. After centrifugation to get rid of the excess emulsifier, the particles could not be redispersed, probably due to the low surface charge. Therefore, base (NaOH) was added, adjusting the pH to a neutral value in order to increase the charges of PMAA (see Figure 27) and make it possible to redisperse the concentrated microcapsules.

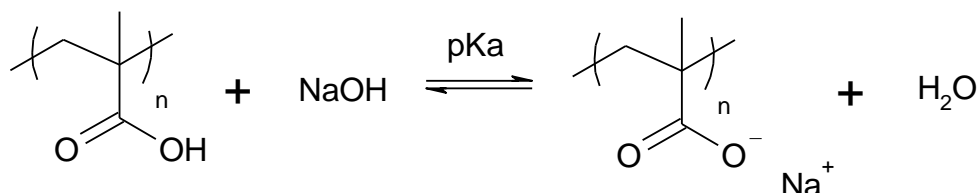


Figure 27. A acid base equilibrium between PMAA and NaOH.

The degree of adsorption of PMAA on the surface of microcapsule could be calculated based on the results obtained from ESCA tests. The structures of PMMA and PMAA are shown in Figure 28.

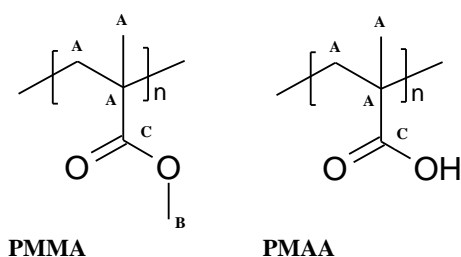


Figure 28. The structures of PMMA and PMAA.

Carbon appears in PMMA in three chemical environments (A, B and C) resulting in three identifiable binding energies for the C1s transition. Each chemical state appears in a proportion of 3:1:1 in the PMMA repeating unit. Oxygen appears in PMMA in two chemical environments resulting in two binding energies for the O1s transition. Each chemical state appears in equal proportions in PMMA molecule. While in the PMAA repeating unit, oxygen appears in the same way as in PMMA, however, carbon only appears in two chemical environments (A and C) with each chemical state appearing in a proportion of 3:1. Therefore the content of carbon in PMMA is higher than that in PMAA, and oxygen in two different chemical environments are always in equal proportions. Based on these, a lot of information can be obtained from the ESCA results.

The elemental composition at the surface of microspheres with PMAA as emulsifier is shown in Table 8 in Appendix IV. The concentration of C1s was higher and the concentration of O1s was lower in the pH-adjusted microsphere than in the pure microsphere. It indicated that pure microsphere had less PMMA and more PMAA due to the higher content of carbon and lower content of oxygen in PMMA compared to PMAA. The existence of Na on the microsphere at pH 7.0 was reasonable since protons are exchanged for sodium counterions during the acid base reaction.

According to the calculations, the sample of pure microsphere (without pH treatment) has less PMMA and more PMAA. This corresponds to the analysis obtained from the elemental composition. The same conclusion can be drawn from the intensity of carbons with different binding energy which is shown in Figure 29. Because carbon B only appears in PMMA, therefore the intensity of peak B can be used to compare the contents of PMMA in two samples. Obviously, pure microsphere has less PMMA.

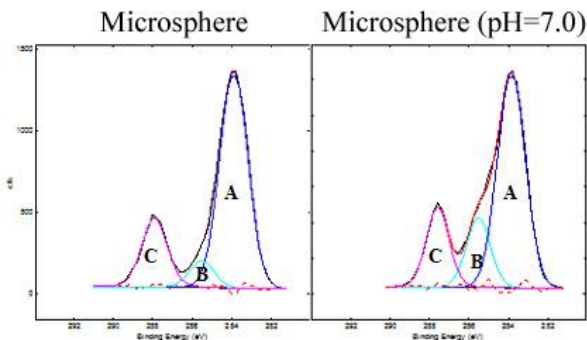


Figure 29. High resolution ESCA spectra of C1s.

Although an increasing bulk pH leads to an increased degree of dissociation, α , according to Figure 27, thus more negative charges on the polymer, it also renders the polyacid more water soluble. The charging of the capsules is therefore counteracted by desorption of the emulsifying polyacid. This explains the lower ζ -potential of the redispersed sample. The desorption of PMAA is displayed in Figure 30 and fitted with a multinomial curve assuming 100% adsorbed amount at low pH and ultimately 0% adsorbed at very high pH values. The calculation of the normalized adsorbed amount of PMAA is explained in Appendix.

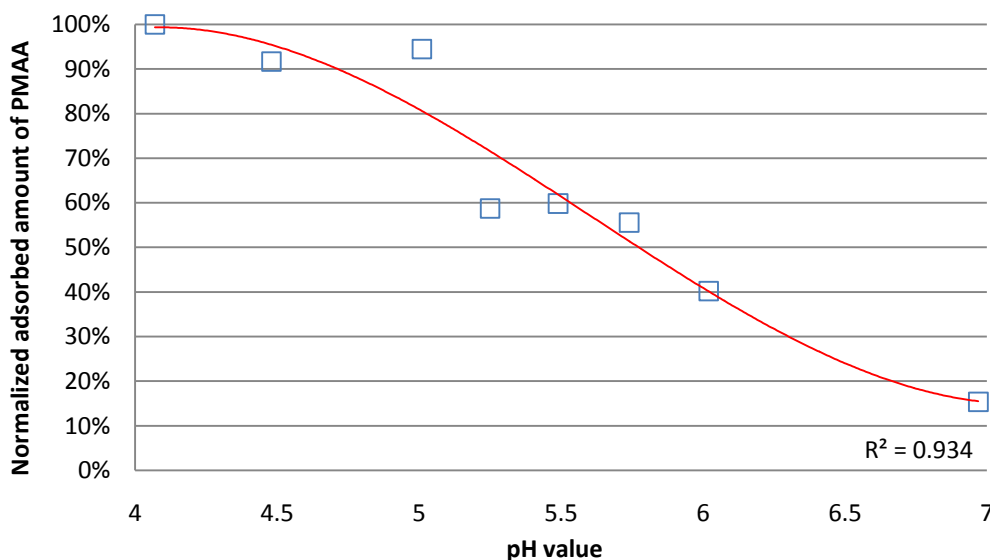


Figure 30. The normalized adsorbed amount of PMAA as a function of increasing pH values.

With the increasing pH values, there was an obvious trend that the content of PMAA gradually decreased. This result was perfectly in correspondence with the theory that increasing pH leads to an increased α (degree of dissociation) and increased water solubility, resulting in polymer desorption and therefore a decreasing surface charge.

Surface modification on colloidal particles

LbL assembly of Polyelectrolytes

The ζ -potential as followed during the adsorption of four polyelectrolyte layers on PMMA(600)-b-PMANa(4600) and TC4-PDADMAC capsules are displayed in Figure 31. The emulsifier itself on the particles is regarded as the first layer.

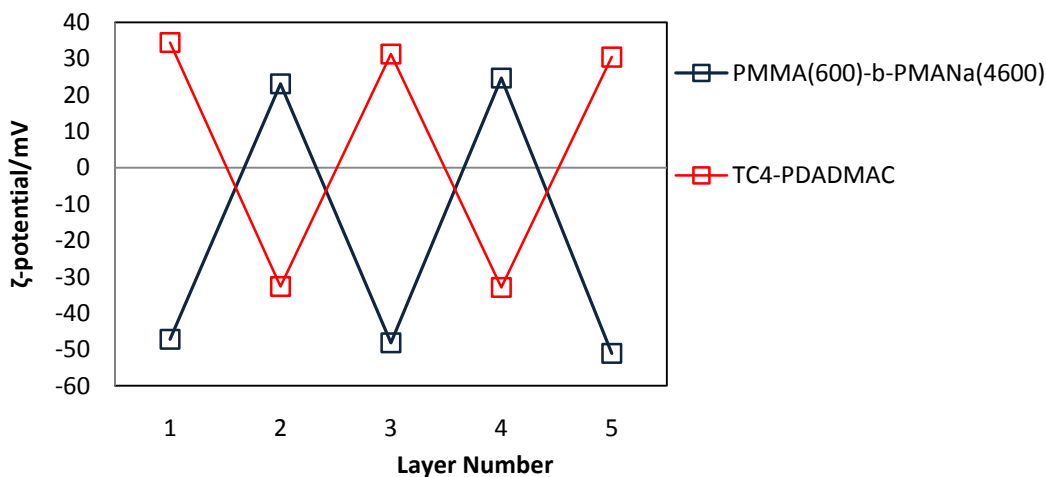


Figure 31. ζ -potential as a function of layer number for particles with PMMA(600)-b-PMANa(4600) and TC4-PDADMAC as emulsifiers respectively.

Regarding the results for multilayers on particles with PMMA(600)-b-PMANa(4600) as emulsifier, the value of ζ -potential started from -47mV for the first layer, followed by +23mV for the PDADMAC layer and -48mV for the PMAANa⁺ layer, and subsequently alternating with almost the same values for the next pair of layers. The difference between each change was around 70mV. The ζ -potential alternates between negative and positive values indicating a successful charge inversion in this system which is sufficient to ensure the adsorption of each layer deposition on the template particles.

Whether the adsorption of each layer of polyelectrolytes is successful or not can also be seen simply by visual observation. If there's precipitation during the adsorption, which suggests the formation of polyelectrolyte complexes, the adsorption is most likely unsuccessful. The existence of polyelectrolyte complexes can be a product of the polyelectrolytes desorbed from the surface and the newly added oppositely charged polyelectrolytes, or there are still excess polyelectrolytes in the suspension after washing, indicating an insufficient washing process.

The same conclusion could be obtained from the ζ -potential values for particles with TC4-PDADMAC as emulsifier. The difference between each change was about 70mV as well. The steadiness in the ζ -potential difference during the LBL assembly of this system suggests that the consecutive adsorption cycles of PDADMAC and PMAANa⁺ can be extended to an indefinite number of layers which obviously helps in fine controlling the shell's thickness and the release of the active substances inside.

Different salt concentrations were used during adsorption for two cases, 1M NaCl for copolymer capsule and 0.5M for TC4 capsule, as mentioned earlier. 0.5M NaCl was used because the TC4 capsule couldn't survive under higher concentration of salt. Salt can screen the charges, thus reduce the repulsion between particles. Too much salt can lead to aggregations of particles. Since TC4 capsule has a lower surface charge, therefore lower concentration of salt was used to avoid aggregations. Another possible reason might be that the steric repulsion was weaker for TC4 capsule since the emulsifiers were most likely flat on the surface, while for copolymer capsule, the emulsifiers were most likely stretched out on the surface.

Table 4. The ζ -potential values of particles with two or three layers.

Emulsifier	ζ -potential/mV		
	Layer 1	Layer 2	Layer3
PMAA	-22.49	+20.00	-
PMMA(4300)-b-PANa(17500)	-34.46	+35.32	-31.15
PMMA(4000)-b-PMANa(9300)	-52.11	+51.36	-

For the other types of block copolymers and PMAA, which have been used to synthesize microcapsules successfully, the LBL assembly of oppositely charged polyelectrolytes on them has been also proved to be successful due to the inversion values of ζ -potential in first two or three layers (Table 4). But for the particles with PMAA as the emulsifier, since PMAA is a very weak polyelectrolyte, the ζ -potential value was around 20mV, relatively lower than those of particles made with other types of emulsifiers.

The charge inversion over increasing layer number for other kinds of microcapsules is shown in Figure 32.

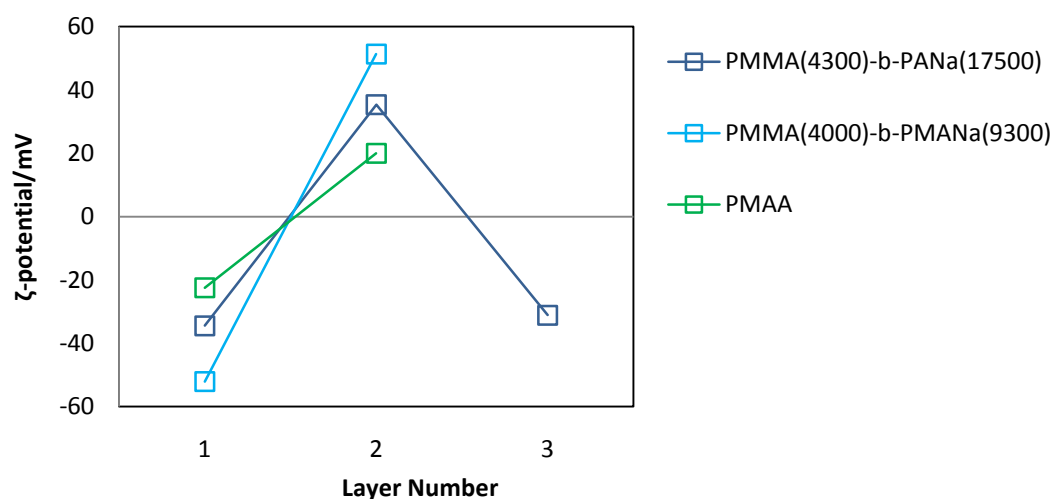


Figure 32. The charge inversion over increasing layer number for other kinds of microcapsules.

Regarding the microcapsules with PMMA(4300)-b-PANa(17500) as emulsifier, even though the surface charge was lower than that of TC4 capsule, they could survive under 1M NaCl during adsorption of polyelectrolytes. This indicated that it was the steric repulsion that played a dominant role in what concentration of salt should be used.

Building lipid bilayers on the surface of microcapsule

Cationic and anionic SUVs were prepared using the method mentioned in Methods section.

The size distribution and ζ -potential results from light scattering for cationic DA(H) SUVs and anionic DSPA SUVs are shown in Appendix V. The size of DA(H) SUVs is around 100nm and the ζ -potential is around 50mV. The size of DSPA SUVs is around 85nm and the ζ -potential is around 44mV.

SUVs prepared using cationic lipid, DA(H), was mixed with a negatively charged microcapsule with PMMA(600)-b-PMANa(4600) as emulsifier adsorbed with two polyelectrolyte layers above the T_m . It turns out to be successful to build this lipid bilayer onto the surface of microcapsule due to the high surface charge, which was around +42mV. However, it became +18mV after the washing step, indicating that desorption of lipid bilayers occurred (see Figure 33).

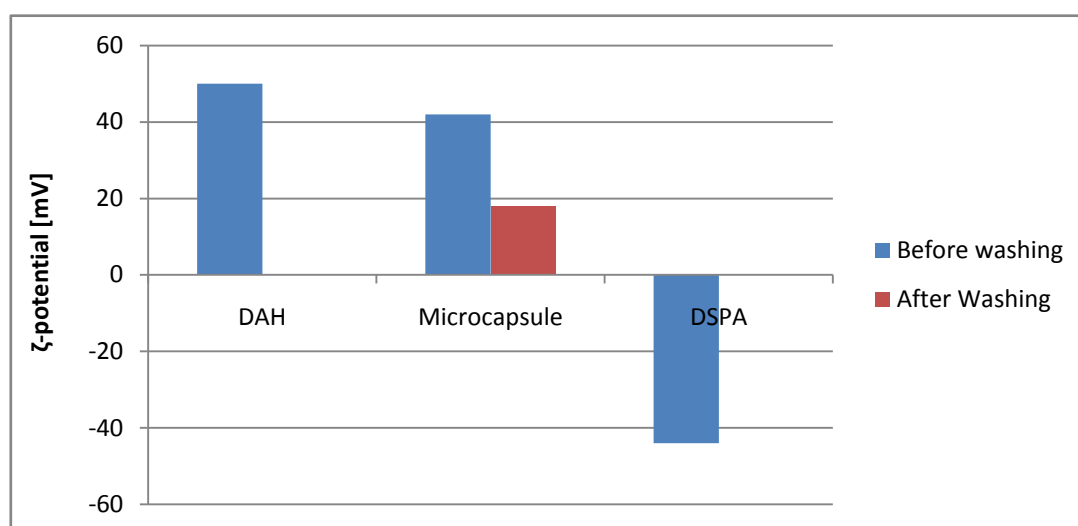


Figure 33. ζ -potential for SUVs of two lipids and adsorption on the microcapsules.

Conclusion

1. Compared with PMAA microcapsules, the microcapsules made with block copolymers and TC4-PDADMAC as emulsifiers had a higher surface charge and there was no problem to redisperse them without excess emulsifier present.
2. PMAA microcapsule was able to be redispersed in water by increasing pH. PMAA was gradually desorbed from the surface leading to aggregation after some days.
3. Microcapsule made with TC4-PDADMAC as emulsifier could not maintain stability for more than a few weeks due to the unfulfilled spreading condition.
4. LbL assembly of polyelectrolytes was proved to be successful for all types of microcapsules synthesized in this work.
5. The steadiness in ζ -potential difference during LbL assembly suggests that the consecutive adsorption cycles of PDADMAC and PMAANa can be extended to an indefinite number of layers.
6. Regarding the particles with PMAA as emulsifier, the ζ -potential was relatively low, indicating that it was not suitable for multilayer assembly.
7. Lipid bilayers could be adsorbed on the surface of microcapsules. However, the washing procedure needs to be improved in order to prevent lipid desorption.

Future work

The future work will focus on the surface modification of microcapsules with other several types of block copolymers as emulsifiers. The washing protocol for microcapsules with adsorbed lipid bilayers needs to be improved. Most importantly, the release rate of biocides from microcapsules will be studied as well, such as the difference of release rate from microcapsules synthesized with different types of emulsifiers, or the difference of release rate from pure microcapsules and microcapsules adsorbed with polyelectrolyte multilayers or lipid bilayers.

Acknowledgement

I'd like to thank Magnus Nydén for giving me the opportunity to do this project, and my supervisor Markus Andersson Trojer for his encouragement and guidance during the whole research. A special thank to Anne Wendel for helping us running several ESCA tests, Christoffer Abrahamsson for helping us taking many nice SEM images, and Staffan Wall who helped me a lot with the microelectrophoresis measurements. I also want to thank Krister Holmberg, Alberta Mok, Lars Nordstierna, Ali Reza Movahedi for their generous help and support, and all those friends who supported me during the completion of this work. Finally, I would like to thank my parents for their unconditional support and patience!

Appendix I

Table 5. All the syntheses of microcapsules in this work.

No.	Emulsifier	wt%	PMMA, wt%	Water volume/ml	Shear rate/rpm	Comments
1	PVA	2.000%	2.000%	200	10000	
2	PDADMAC	2.000%	2.000%	200	10000	
3	PDADMAC	2.000%	2.000%	200	10000	
4	PMAA	1.275%	1.275%	200	10000	
5	PDADMAC	2.000%	2.000%	200	10000	1M NaCl
6	PMAA	0.6375%	1.275%	200	10000	pH after
7	PMAA	0.6375%	1.275%	200	10000	pH before
8	PMAA	1.275%	1.275%	50	10000	
9	PMAA	0.400%	0.400%	50	10000	Reduced DCM and acetone
10	PMAA	0.400%	0.400%	50	10000	
11	600-4600 ^a	0.400%	0.400%	50	7500	
12	5500-6200 ^b	0.400%	0.400%	50	7500	
13	4300-17500 ^c	0.400%	0.400%	50	7500	
14	4000-9300 ^d	0.400%	0.400%	50	7500	
15	18000-57400 ^e	0.400%	0.400%	50	7500	
16	PVA	0.400%	0.400%	50	7500	
17	18000-57400	0.050%	0.400%	50	7500	
18	TC4/PDADMAC	0.050%/0.100%	0.400%	50	7500	
19	TC4/PDADMAC	0.0125%/0.100%	0.400%	50	7500	
20	TC4/PDADMAC	0.005%/0.100%	0.400%	50	7500	

^a PMMA(600)-b-PMAANa(4600), ^b PMMA(5500)-b-PAANa(6200), ^c PMMA(4300)-b-PAANa(17500), ^d PMMA(4000)-b-PMAANa(9300), ^e PMMA(18000)-b-PAANa(57400).

Appendix II

Table 6. The experimental data of batches synthesized under different conditions.

Wt% of PMAA	Volume of water/ml (batch size)	Shear rate/rpm	Size/ μm
1.275%	200	10000	6
1.275%	50	10000	1
0.400%	50	10000	2
0.400%	50	7500	3
0.400%	100	7500	4-5

Appendix III

Table 7. The ζ -potential results of all types of microcapsules.

Emulsifier	ζ -potential/mV initial	ζ -potential/mV redispersed
PMAA	-29.46 ± 1.6	-22.49 ± 3.4^a
PMMA(600)-b-PMANa(4600)	-54.77 ± 4.4	-47.24 ± 4.2
PMMA(4300)-b-PANa(17500)	-31.94 ± 2.7	-34.46 ± 3.8
PMMA(4000)-b-PMANa(9300)	-58.07 ± 3.7	-52.11 ± 3.6
PMMA(18000)-b-PANa(57400)	-42.50 ± 3.6	—— ^b
TC4-PDADMAC	$+36.87 \pm 3.8$	$+37.70 \pm 2.4$

^a the pH of the suspension was adjusted to 7.0;

^b failed to be washed by centrifugation due to its high viscosity.

Appendix IV

Table 8. The atomic concentration results of PMAA microspheres.

Samples	C1s [0.314]	O1s [0.733]	S2p [0.717]	Na1s [1.102]
Microsphere	68.48	31.18	0.34*	-
Microsphere (pH=7.0)	71.24	27.66	-	1.10

* The existence of atom S might be caused by contamination.

The information of carbon and oxygen bands in different chemical environments is listed in Table 9. The area% of oxygen of A and B bands for both pure and pH-adjusted microspheres was almost the same (around 50%), which corresponded with the earlier analysis. Based on the values of area% of carbon in three chemical environments and the proportions of them in PMMA and PMAA molecules, the content of two polymers can be calculated out.

Table 9. The information of C and O bands in different chemical environments.

	Atom	Band	Pos	FWHM*	%Area
Microsphere	C	A	283.89	1.68	71.32
		B	285.52	1.47	7.41
		C	287.92	1.50	21.27
	O	A	531.08	1.65	50.72
		B	532.60	1.65	49.28
Microsphere (pH 7.0)	C	A	283.84	1.65	62.97
		B	285.52	1.41	17.44
		C	287.58	1.34	19.59
	O	A	530.88	1.60	51.12
		B	532.50	1.60	48.88

* the full width at half maximum.

The calculating method is illustrated here taking pure microsphere as example. Because carbon B only appears in PMMA and the ratio between carbon B and C in PMMA is 1:1, so the area% of carbon C in PMMA is 7.41%. Since carbon C appears both in PMMA and PMAA, the area% of carbon C in PMAA is (21.27%-7.41 %)= 13.86%. Therefore the content of PMMA and PMAA can be calculated based on the area% values of carbon C of both polymers. We assumed that only these two polymers existed in the sample, then the content of PMMA is (7.41%/ 21.27 %)= 34.8% and the content of PMAA is (13.86%/ 21.27 %)= 65.2%. Using this method to calculate the composition in the sample of pH-adjusted microsphere, the results are: the content of PMMA is 89.0% and the content of PMAA is 11.0%.

The content of PMMA and PMAA were calculated using the same method as mentioned earlier. The area% of different C bands, the calculated results of content of PMAA, and normalized adsorbed amount of PMAA based on the content of PMAA are listed in Table 10.

Table 10. The area% of different C bands and the calculation results of content of PMMA and PMAA.

Band	pH value								
	% Area	4.07	4.48	5.01	5.25	5.49	5.74	6.02	6.97
A		67.94	68.90	68.30	66.73	68.00	67.31	64.58	63.91
B		10.06	10.43	10.43	13.50	12.92	13.46	15.55	17.26
C		22.00	21.27	21.27	19.77	19.08	19.22	19.87	18.83
Content of PMAA		54%	49.5%	51%	31.7%	32.3%	30%	21.7%	8.3%
Normalized adsorbed amount of PMAA		100%	92%	94%	59%	60%	56%	40%	15%

A series of microsphere samples with increasing pH values were then prepared and tested by ESCA. The content of PMMA and PMAA were calculated using the same method as mentioned earlier. The area% of different C bands, the calculated results of content of PMAA, and normalized adsorbed amount of PMAA based on the content of PMAA are listed in Table 10. Based on the calculation results in Table 10, the normalized adsorbed amount of PMAA as a function of increasing pH values was marked in Figure 30. A curve was drawn to display the trend of the adsorbed amount of PMAA over pH values.

Appendix V

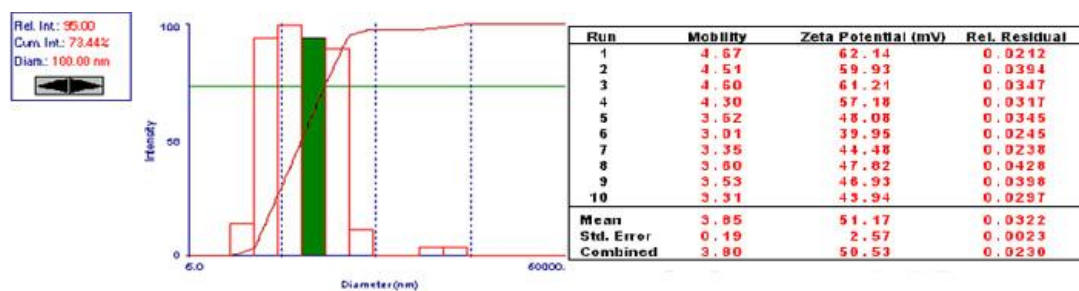


Figure 34. The size distribution and Zeta potential results for DA(H) SUVs.

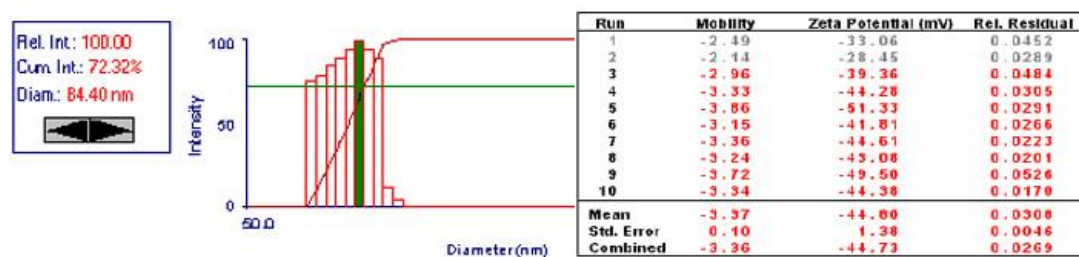


Figure 35. The size distribution and Zeta potential results for DSPA SUVs.

References

1. Rachel Parks, Marion Donnier-Marechal, Patricia E. Frickers, Andrew Turner, James W. Readman. *Marine Pollution Bulletin*. 60, **2010**, 1226-1230.
2. *Marine paint annual report 2009*. Gothenburg, **2009**.
3. L. D. Chambers, K. R. Stokes, F. C. Walsh, R. J. K. Wood. *Surface & Coatings Technology*. 201, **2006**, 3642-3652.
4. Markus Andersson Trojer. Thesis for the degree of licentiate of engineering. Chalmers University of Technology, Gothenburg, **2009**.
5. A. Terlizzi, S. Frascchetti, P. Gianguzza, M. Faimali, F. Boero. *Aquat. Conserv. Mar. Freshw. Ecosyst.* 11, **2001**, 311.
6. J. Lewis. Hull fouling as a vector for the translocation of marine organisms: Report 1 and 2, Dept. of Agriculture, Fisheries and Forestry-Australia, Marine Science and Ecology Pty. Ltd. Commonwealth of Australia. **2002**.
7. F. FaÿI. Linossier, G. Legendre , K. Vall é-R éhel. *Macromol. Symp.* 272, **2008**, 45.
8. Tam ász Szab ó, L ívia Moln ár-Nagy, J ános Bogn ár, Lajos Nyikos, Judit Telegdi. *Progress in Organic Coatings*. 72, **2011**, 52-57.
9. K. Shekhar, M. Naga Madhu, B. Pradeep, David Banji. *International Journal of Pharmaceutical Sciences Review and Research*. **2010**, 5(2), 58-62.
10. Risch, S.; et al. In Encapsulation and Controlled Release of Food Ingredients. ACS Symposium Series. American Chemical Society: Washington, DC, 1995.
11. H. G. Bungenberg de Jong. *Colloid Science (Ed. H.R. Kruyt)*, Elsevier. Through, Swapan Kumar Ghosh, Functional Coatings and Microencapsulation: A General Perspective. **1949**, 232–258.
12. Rama Dubey; T. C. Shami; K. U. Bhasker Rao. *Defence Science Journal*. **2009**, 59(1), 82-95.
13. Sergio Freitas; Hans P. Merkle; Bruno Gander. *Journal of Controlled Release*. **2005**, 102, 313-332.
14. G. Bungenberg de Jong, H. Kruyt. *Prog. Kungl. Ned. Acad. Wetensch.* **1929**, 32, 849-856.
15. Loxley, A.; Vincent, B. J. *Colloid Interface Sci.* **1998**, 208, (1), 49-62.
16. Application of Layer-by-Layer Assembled Nanoparticle Composite Films. Oxana Tchoul, Department of Chemistry, Oklahoma State University.
17. Gero Dechor. *Abstracts of Papers, 223rd ACS National Meeting, Orlando, FL, United States, April 7-11. 2002*, 016.
18. Michael W. Davidson, Florida State University, Darkfield Microscopy, 1998, [retrieved: 2011:10:03], <http://micro.magnet.fsu.edu/primer/techniques/darkfieldindex.html>
19. Thomas J. F., Michael W. Davidson, National High Magnetic Field Lab, Darkfield microscopy, 2011, [retrieved: 2011:10:03], http://en.wikipedia.org/wiki/Dark_field_microscopy
20. Microscope Master, Microscope Reviews and Microscopy Research, Dark Field Microscope, [retrieved: 2011:10:03], <http://www.microscopemaster.com/dark-field-microscope.html>
21. A. V. Delgado, et al. *IUPAC, Pure and Applied Chemistry*. **2005**, 77 (10), 1753-1805.
22. Shin-ichi Nagaoka. A short history of three chemical shifts. *J. Chem. Educ.* **2007**, 84 (5), p801.
23. Danilo D. Lasic. Liposomes in Gene Delivery. CRC Press LLC, 1997.
24. Mohamed, A.; Trickett, K.; Chin, S. Y.; Cummings, S.; Sagisaka, M.; Hudson, L.; Nave, S.; Dyer, R.; Rogers, S. E.; Heenan, R. K.; Eastoe, J. *Langmuir*. **2010**, 26, (17), 13861-13866.
25. Gero Decher. *Science*. **1997**, 277, 1232-1237.
26. Gleb B. Sukhorukov; Helmuth M öhwald; et al. *Colloids Surfaces A: Physicochem. Eng. Aspects*.

- 1998**, 137, 253-266.
27. Malcolm N. Jones. *Advances in Colloid and Interface Science*. **1995**, 54, 93-128.
 28. A. D. Bangham. Liposomes: realizing their promise. *Hospital Practice*. **1992**, 27(12), 51-6, 61-2.
 29. A. D. Bangham. Liposomes: the Babraham connection. *Chemistry and Physics of Lipids*. **1993**, 64, 275-285.
 30. F. Szoka, D. Papahadjopoulos. *Proc. Nat. Acad. Sci.* **1978**, 75, 4194.
 31. L. D. Mayer, M. J. Hope, P. R. Cullis. *Biochim. Biophys. Acta*. **1986**, 858, 161.
 32. G. Strauss. *J. Soc. Cosmet. Chem.* **1989**, 40, 51.
 33. D. Papahadjopoulos. Liposomes and Their Uses in Biology and Medicine. *Ann. N. Y. Acad. Sci.* **1978**, 308.
 34. M. N. Jones. Biochemical Thermodynamics. Second Edition, Chapter 5, Elsevier, Amsterdam, **1988**.
 35. C. Groth, K. Tollgerdt, M. Nydén. *Colloids and Surfaces A: Physicochem. Eng. Aspects*. **2006**, 281, 23-34.
 36. GuoTao Chao, HongXin Deng, et al. *Journal of Polymer Research*. 2006, 13(5), 349-355.
 37. Mortimer Abramowitz, Michael W. Davidson. Introduction to Microscopy, 2004, [retrieved: 2011:12:01], <http://micro.magnet.fsu.edu/primer/anatomy/introduction.html>
 38. Grahame D. C. *Chemical review*. **1947**, 41 (3), 441-501.
 39. LEO ULTRA 55 FEG, SEM, Instrumentation, Applied physics, Chalmers University of Technology, 2007, [retrieved: 2011:12:13], <https://www.chalmers.se/ap/EN/research/microscopy-microanalysis/instrumentation/sem/leo-ultra-55-feg>
 40. E. Pasani, E. Fattal, J. Paris, C. Ringard, V. Rosilio, N. Tsapis. *Journal of Colloid and Interface Science*. **2008**, 326,66.
 41. C. A. Finch, R. Bodmeier. Microencapsulation, Wiley-VHC Verlag GmbH&Co. **2002**.
 42. P. J. Dowding, R. Atkin, B. Vincent, P. Bouillot. *Langmuir*. **2004**, 20, 11374.
 43. S. Moya, L. Dähne, A. Voigt, S. Leporatti, E. Donath, H. Möhwald. *Colloids and Surfaces A: Physicochemical and Engineering Aspects*. **2001**, 183-185, 27-40.
 44. K. Holmberg, B. Jönsson, B. Kronberg, B. Lindman. Surfactants and Polymers in Aqueous Solution, 2nd edition. John Wiley & Sons Ltd. 2003.
 45. [retrieved: 2011:09:15], <http://noopurmandrek.files.wordpress.com/2010/09/lipo1.jpg>
 46. Ling Zhang, Hiroyuki Nakamura, Changi Lee, Masato Uehara, Hideaki Maeda. IOP Conf. Series: Materials Science and Engineering. **2011**, 18, 082027.
 47. Gero Decher, Joseph B. Schlenoff. Multilayer Thin Films: Sequential Assembly of Nanocomposite Materials, Wiley-VCH Verlag GmbH&Co. KGaA, Weinheim. **2003**.
 48. Nam-Joon Cho, Curtis W. Frank, Bengt Kasemo, Fredrik Höök. *Nature Protocols*. **2010**, 5 (6), 1096-1106.